北京计算科学研究中心 11/12/2020

非平衡态下缺陷性质的第一性原理计算

陈时友
华东师范大学 物理与电子科学学院

极化材料与器件教育部重点实验室
Key Laboratory of Polar Materials and Devices, Ministry of Education

半导体晶格中的点缺陷

$Cu_2ZnSnSe_4$

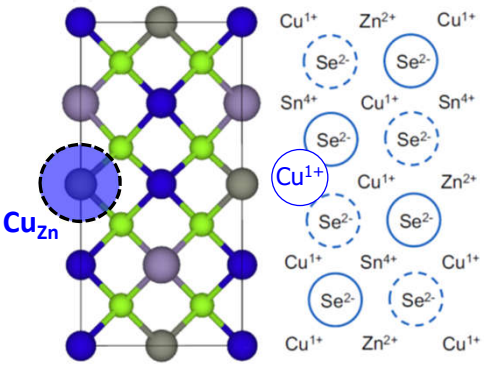

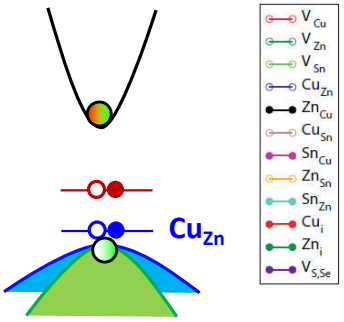

平衡态下缺陷浓度

EIGHTH EDITION
Introduction to Solid State Physics
CHARLES KITTEL

CHAPTER 20: POINT DEFECTS

The probability that a given site is vacant is proportional to the Boltzmann factor for thermal equilibrium: $P = \exp(-E_V/k_BT)$, where E_V is the energy required to take an atom from a lattice site inside the crystal to a lattice site on the surface. If there are N atoms, the equilibrium number n of vacancies is given by the Boltzmann factor

$$\frac{n}{N-n} = \exp(-E_V/k_BT) \ . \qquad (1)$$

If $n \ll N$, then

$$n/N \cong \exp(-E_V/k_BT) \ . \qquad (2)$$

If $E_V \approx 1$ eV and $T \approx 1000$ K, then $n/N \approx e^{-12} \approx 10^{-5}$.

辐照下的缺陷

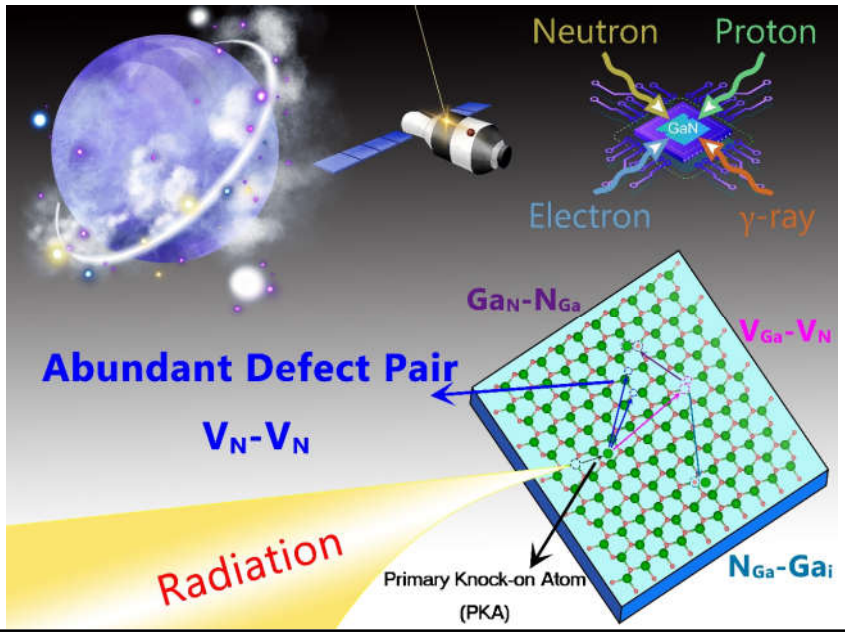

科学问题：缺陷的研究和调控在方法上仍有困难

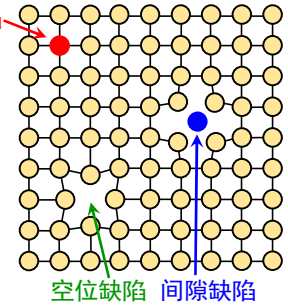

◆ 实验挑战：难以直接观测

浓度低：10^{-7}-10^{-4} (10^{15}- 10^{18} cm^{-3})

多种缺陷共存，难以区分，需要猜测

◆ 理论挑战：难以精确计算模拟，计算误差大，过程复杂

有限超原胞导致的误差（精确计算需考虑百万-千万原子）

缺陷种类和构型繁多，交换关联势近似，都导致误差

Zhang *et al.*, Phys. Rev. Lett. 110, 166404 (2013)
Freysoldt *et al.*, Rev. Mod. Phys. 86, 253 (2014)
Grasser *et al.*, Microelectronics Reliability 87, 286 (2018)

提纲

1. 计算辐照下可能产生的各种缺陷的平衡态性质
   形成能、能级和载流子俘获截面

2. 模拟辐照下化学键的断裂和缺陷形成过程

缺陷形成能（电中性）

$$\Delta H_f(\alpha, q=0) = E(\alpha, q=0) - E(host) + \sum n_i(\mu_i + E_i)$$

移除的原子数n_i　原子化学势 μ_i

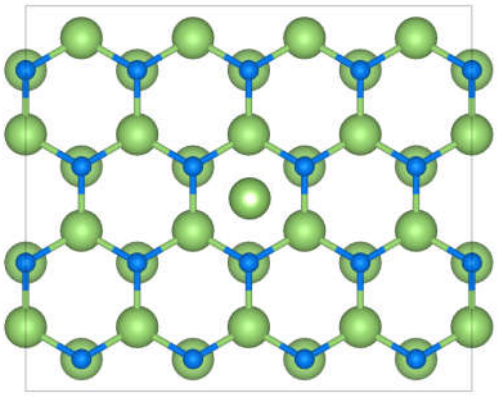

Ga单质

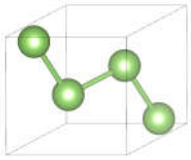

$$\mu_{Ga} + E_{(Ga)} \leq E_{(Ga)}$$
$$\mu_{Ga} \leq 0$$

缺陷形成能（缺陷带电）

$$\Delta H_f(\alpha, q) = E(\alpha, q) - E(host) + \sum n_i(\mu_i + E_i)$$
$$+q(E_F + E_V + \Delta V)$$

电子化学势 E_F （费米能级）

缺陷的带电状态与费米能级有关

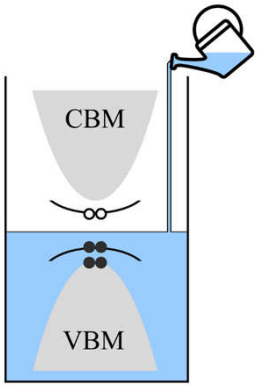

原子的化学势以E_i为基准变化

原子化学势 μ_i反映了该原子在体系中的“贫”或“富”。

电子的化学势以E_V为基准变化

电子化学势 E_F反映了电子在该体系中的“贫”或“富”。

缺陷形成能的计算

$$\Delta H_f(\alpha,q) = \underset{①}{E(\alpha,q)} - \underset{②}{E(host)} + \sum \underset{③\ ④}{n_i(\mu_i + E_i)} + \underset{⑤⑥\ ⑦\ ⑧}{q(E_F + E_V + \Delta V)}$$

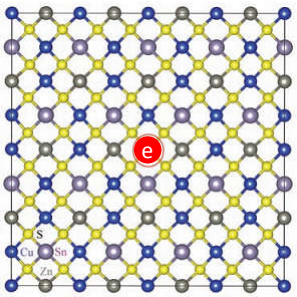

① —含缺陷超胞的总能
② —无缺陷超胞的总能
③ —原子化学势
④ —元素单质相的总能
⑤ —可能的带电状态
⑥ —费米能级
⑦ —价带顶的能量
⑧ —静电势修正项

Semiconductor Defect Ab initio Simulation Code

SDASC

1. 自动确定组成元素和掺杂元素的热力学化学势范围（基于材料基因数据库）
2. 自动产生本征缺陷、杂质及复合缺陷的构型
3. 自动提交第一性原理计算并处理数据
4. 自动计算缺陷形成能和缺陷能级
5. 自动完成镜像电荷、带隙等修正
6. 自动动态计算载流子浓度与费米能级
7. 自动计算高浓度复合中心缺陷的载流子俘获截面

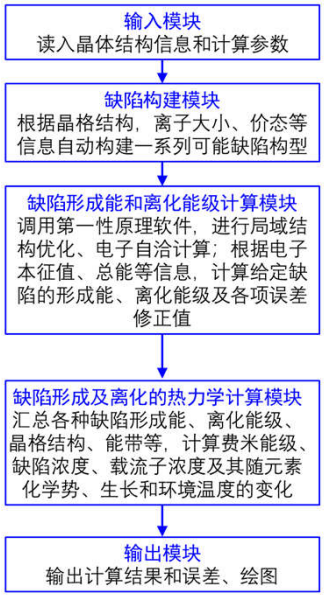

SDASC程序的三个模块

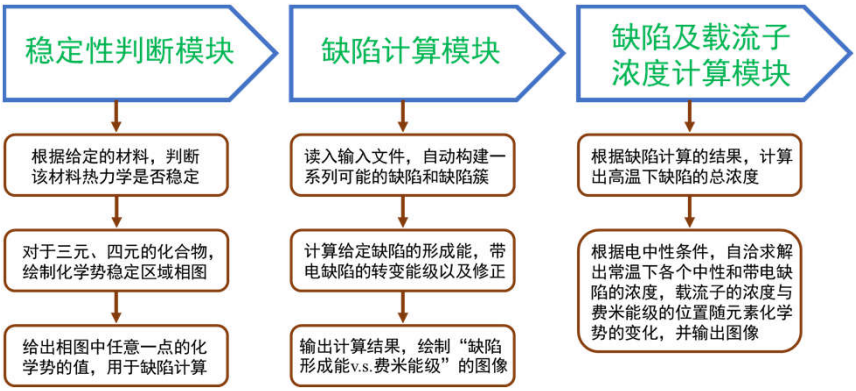

$$\Delta H_f(\alpha,q) = \underset{①}{E(\alpha,q)} - \underset{②}{E(host)} + \sum \underset{③}{n_i}(\underset{④}{\mu_i} + \underset{⑤⑥}{E_i}) + \underset{⑦}{q}(\underset{⑧}{E_F} + E_V + \Delta V)$$

化学势稳定区域的判断

$$\Delta H_f(\alpha,q) = \underset{①}{E(\alpha,q)} - \underset{②}{E(host)} + \sum \underset{③}{n_i}(\underset{④}{\mu_i} + \underset{⑤⑥}{E_i}) + \underset{⑦}{q}(\underset{⑧}{E_F} + E_V + \Delta V)$$

Limit to the element chemical potentials

$$2Cu + Zn + Sn + 4S \rightarrow Cu_2ZnSnS_4$$

$\Delta H_f(Cu_2ZnSnS_4)$
Compound formation enthalpy

Under equilibrium:

$$2\mu_{Cu} + \mu_{Zn} + \mu_{Sn} + 4\mu_S = \Delta H_f(Cu_2ZnSnS_4)$$

No secondary compounds:

$$\mu_{Cu} + \mu_S < \Delta H_f(CuS)$$
$$2\mu_{Cu} + \mu_S < \Delta H_f(Cu_2S)$$
$$\mu_{Zn} + \mu_S < \Delta H_f(ZnS)$$
$$\mu_{Sn} + \mu_S < \Delta H_f(SnS)$$
$$\mu_{Sn} + 2\mu_S < \Delta H_f(SnS_2)$$
$$2\mu_{Cu} + \mu_{Sn} + 3\mu_S < \Delta H_f(Cu_2SnS_3)$$

No elemental phase:

$$\mu_{Cu} < 0$$
$$\mu_{Zn} < 0$$
$$\mu_{Sn} < 0$$
$$\mu_S < 0$$

Narrow stable region in chemical potential space

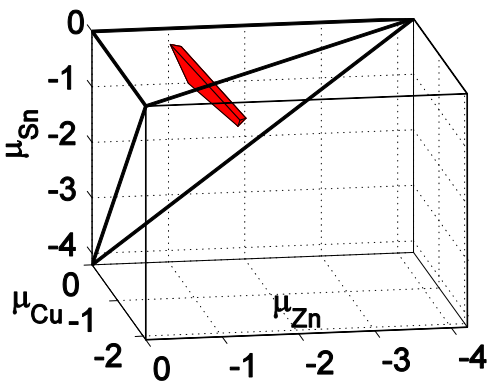

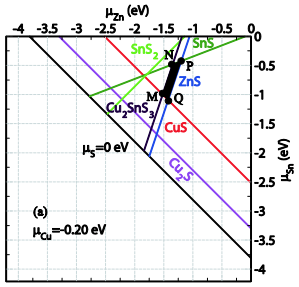

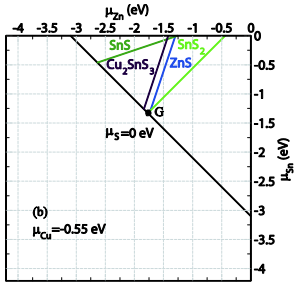

- Narrow stable region.
- ZnS, CuS, SnS form very easily.
- Difficult to synthesize stoichiometric Cu_2ZnSnS_4

$Cu_2Zn-IV-VI_4$ (IV = Si, Ge, Sn, Pb, and Ti, Zr, Hf,

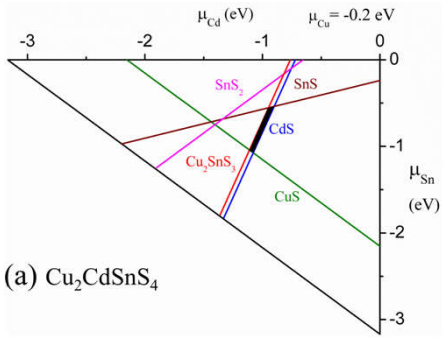

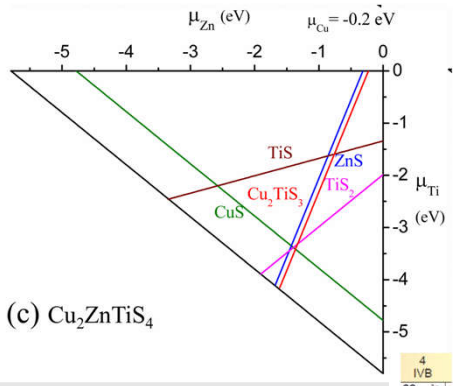

compd.	phase separation	ΔE	ref.
Cu_2ZnSnS_4	$Cu_2S + ZnS + SnS_2$	0.56	40
	$2CuS + ZnS + SnS$	0.40	36
	$Cu_2SnS_3 + ZnS$	0.08	35
Cu_2CdSnS_4	$Cu_2S + CdS + SnS_2$	0.51	32
	$2CuS + CdS + SnS$	0.35	33
	$Cu_2SnS_3 + CdS$	0.03	41
Cu_2HgSnS_4	$Cu_2S + HgS + SnS_2$	0.56	38
	$2CuS + HgS + SnS$	0.37	39
	$Cu_2SnS_3 + HgS$	0.08	

compd.	phase separation	ΔE	ref
Cu_2ZnTiS_4	$Cu_2S + ZnS + TiS_2$	0.15	
	$2CuS + ZnS + TiS$	1.14	
	$Cu_2TiS_3 + ZnS$	−0.05	
Cu_2ZnZrS_4	$Cu_2S + ZnS + ZrS_2$	−0.27	
	$2CuS + ZnS + ZrS$	1.20	
	$Cu_2ZrS_3 + ZnS$	−0.03	
Cu_2ZnHfS_4	$Cu_2S + ZnS + HfS_2$	−0.40	
	$2CuS + ZnS + HfS$	1.73	
	$Cu_2HfS_3 + ZnS$	0.04	

C. Wang et al., Chem. Mater. 26 3411 (2014)

应用1：确定了980种双钙钛矿结构半导体的稳定性

Chemical Trends in the Thermodynamic Stability and Band Gaps of 980 Halide Double Perovskites: A High-Throughput First-Principles Study

Tao Zhang, Zenghua Cai, and Shiyou Chen*

Cite This: *ACS Appl. Mater. Interfaces* 2020, 12, 20680−20690 Read Online

$Rb_2AgInBr_6$

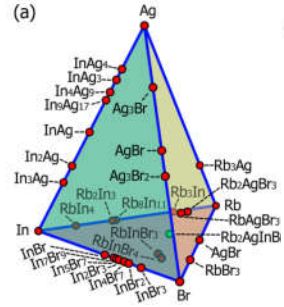

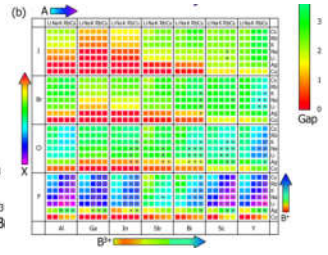

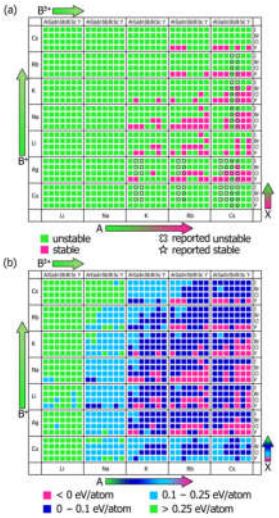

直接调用材料基因组数据库

缺陷构型的构建

$$\Delta H_f(\alpha,q) = E(\alpha,q) - E(host) + \sum n_i(\mu_i + E_i) + q(E_F + E_V + \Delta V)$$

① ② ③ ④ ⑤ ⑥ ⑦ ⑧

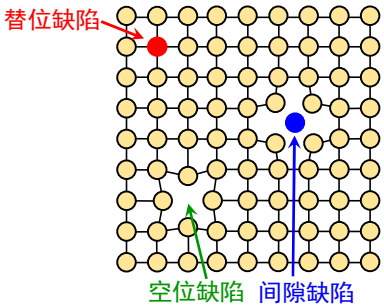

- 空位和替位：考虑不等价原子位置
- 间隙：随机大量结构

施主-受主相互补偿缺陷簇

1. 计算所有的点缺陷的形成能，区分出施主和受主缺陷
2. 将浓度比较高的施主和受主缺陷组合，形成复合缺陷簇

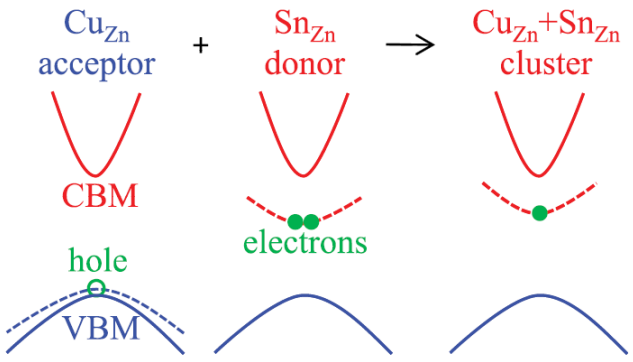

Chen et al. *Appl. Phys. Lett.* **101**, 223901 (2012)

本征缺陷、杂质组成的缺陷-杂质簇

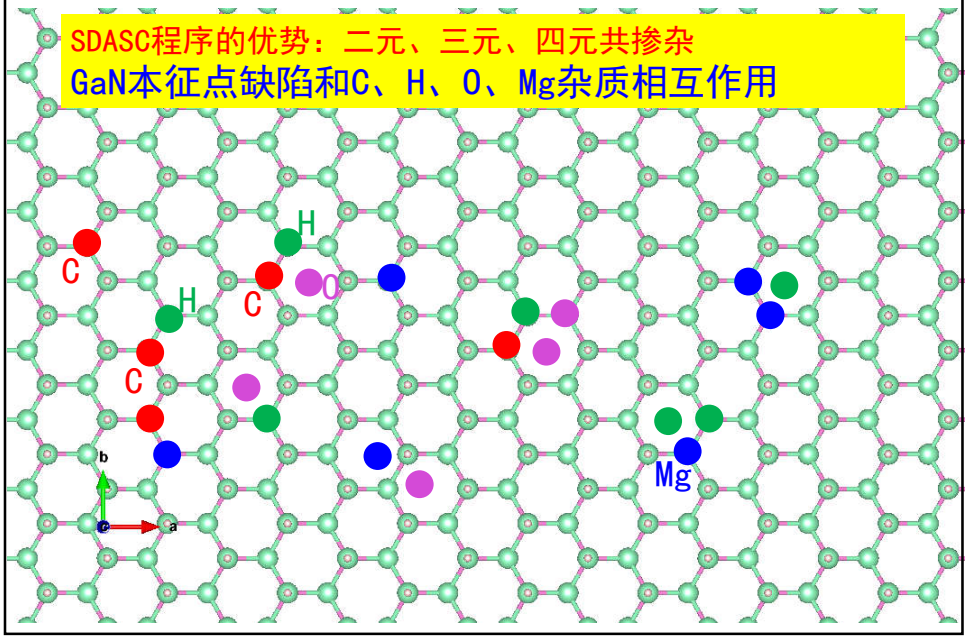

程序应用实例1

SDASC

半导体缺陷第一性原理计算程序

(**S**emiconductor **D**efect **A**b initio **S**imulation **C**ode)

GaN本征点缺陷 （HSE计算）

npj Computational Materials 3, 12 (2017)

REVIEW ARTICLE OPEN

Computationally predicted energies and properties of defects in GaN

John L. Lyons and Chris G. Van de Walle

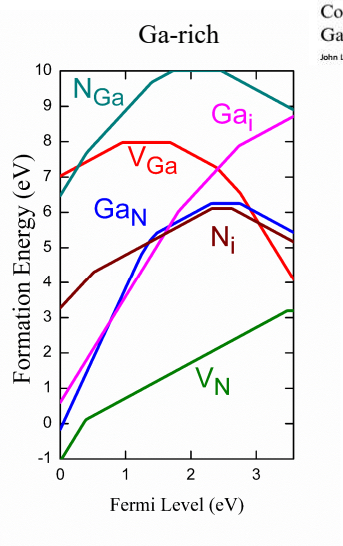

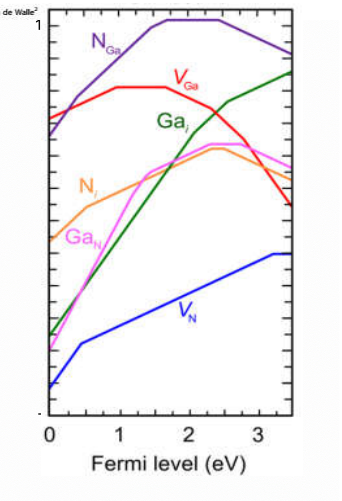

缺陷对

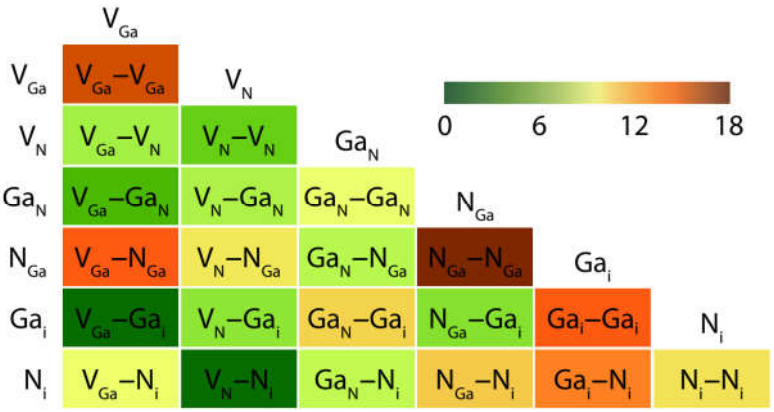

N空位对

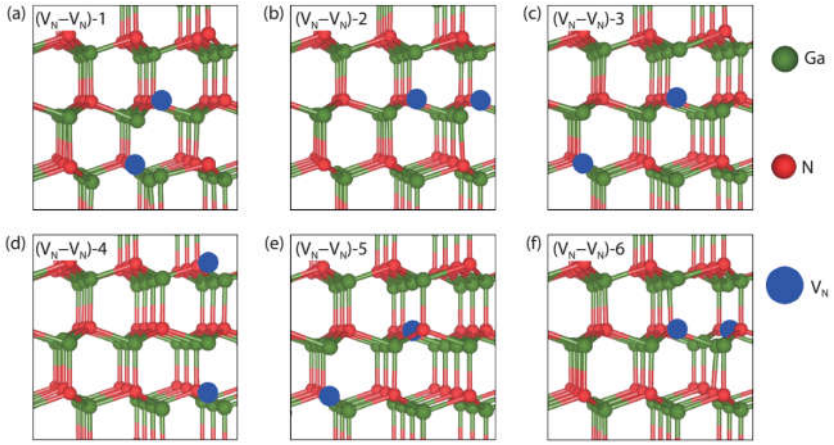

Defect-pair configurations	Initial distance (Å)	Formation energy (eV) PBE-relaxed	Formation energy (eV) HSE-relaxed
$(V_N–V_N)$-1	3.18	4.67	4.58
$(V_N–V_N)$-2	3.19	4.90	4.81
$(V_N–V_N)$-3	4.51	6.83	6.39
$(V_N–V_N)$-4	5.18	6.72	6.57
$(V_N–V_N)$-5	5.52	6.85	6.42
$(V_N–V_N)$-6	5.53	6.85	6.41

GaN本征点缺陷对的形成能

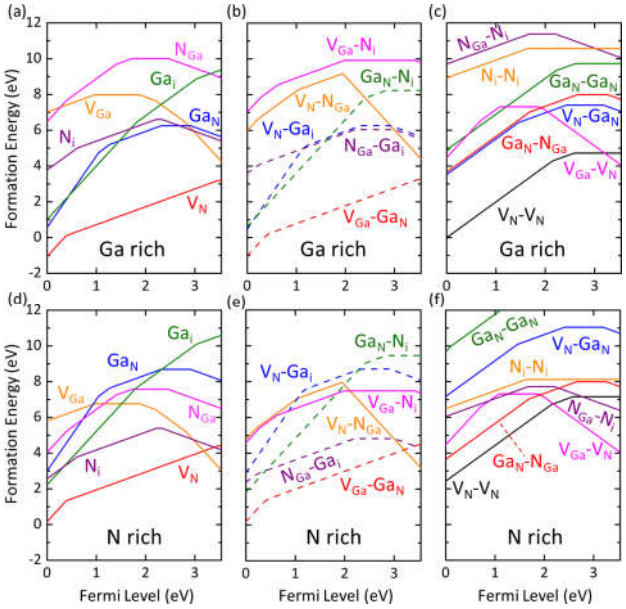

GaN本征点缺陷对的离化能级

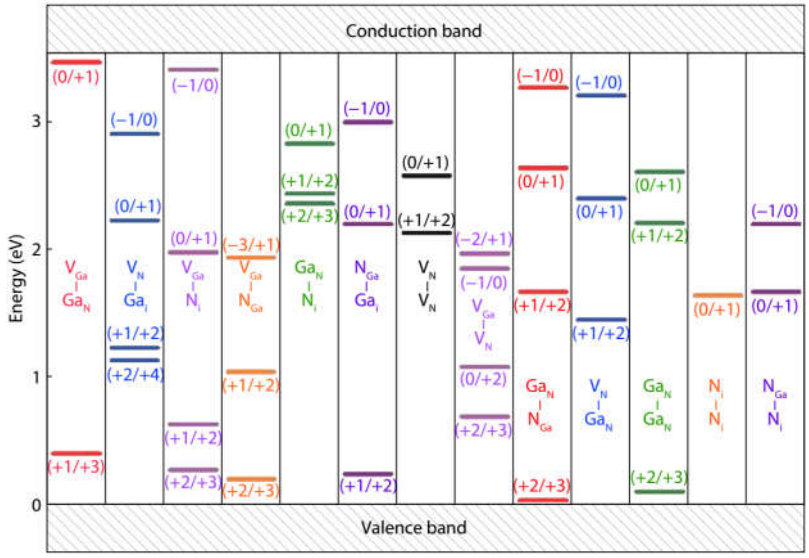

Journal of Semiconductors 41, 032104 (2020)

辐照下GaN中缺陷对

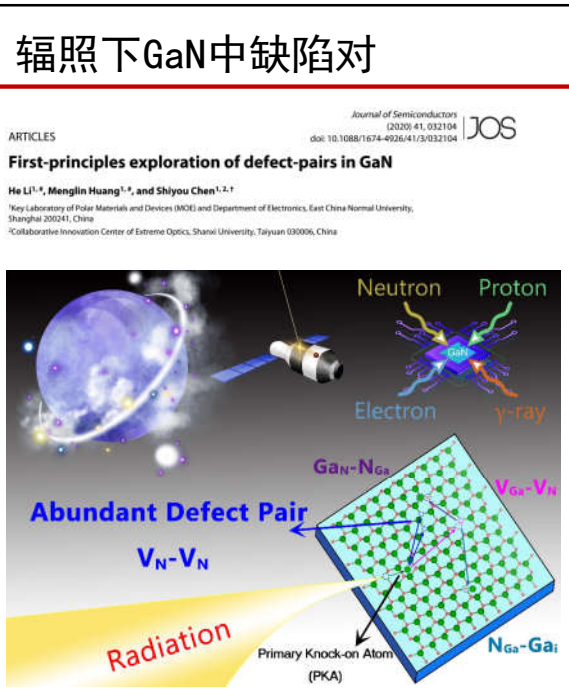

ARTICLES

Journal of Semiconductors (2020) 41, 032104 doi: 10.1088/1674-4926/41/3/032104 JOS

First-principles exploration of defect-pairs in GaN

He Li[1, †], Menglin Huang[1, †], and Shiyou Chen[1, 2, †]

[1]Key Laboratory of Polar Materials and Devices (MOE) and Department of Electronics, East China Normal University, Shanghai 200241, China

[2]Collaborative Innovation Center of Extreme Optics, Shanxi University, Taiyuan 030006, China

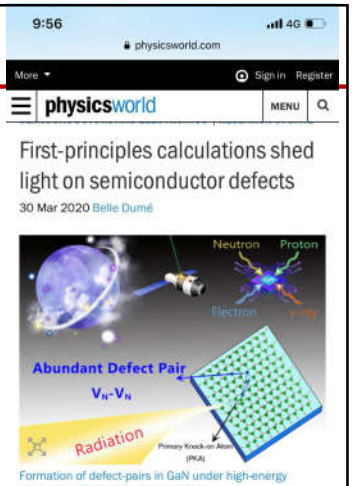

Formation of defect-pairs in GaN under high-energy particle irradiation. Courtesy: S Chen

Gallium nitride (GaN) is the world's second-favourite semiconductor, present in devices ranging from light-emitting diodes and photodetectors to high-temperature electron mobility transistors. When these devices are exposed to irradiation from high-energy particles – as they often are in fields such as satellite communications, aerospace, defence and the nuclear industry – they are prone to developing

Mg、H杂质与本征缺陷形成的缺陷簇

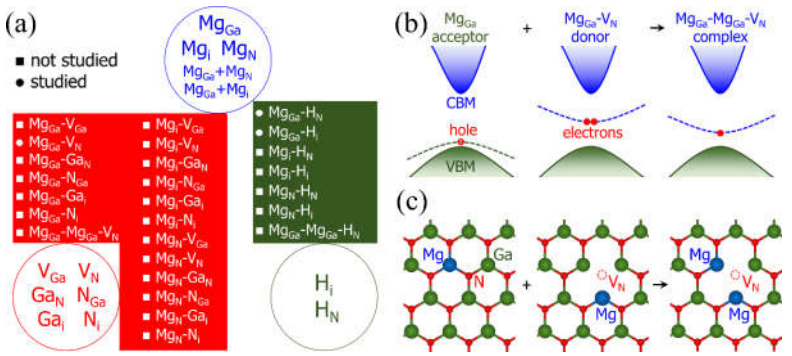

大部分无人算过

Mg_{Ga}-Mg_{Ga}-V_N、Mg_{Ga}-Mg_{Ga}-H_N

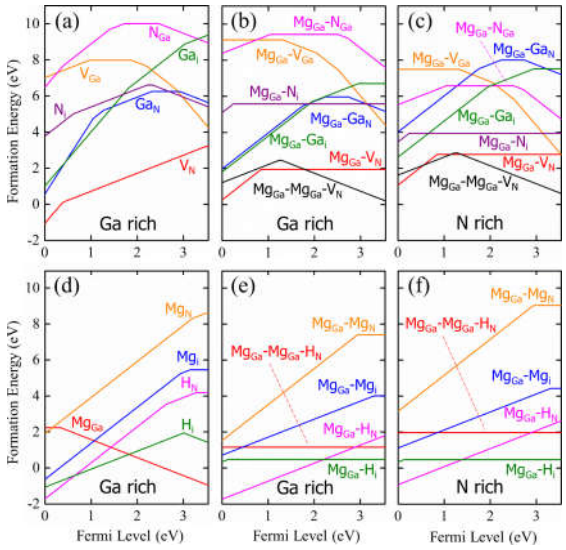

unpublished

Mg_{Ga}-Mg_{Ga}-V_N

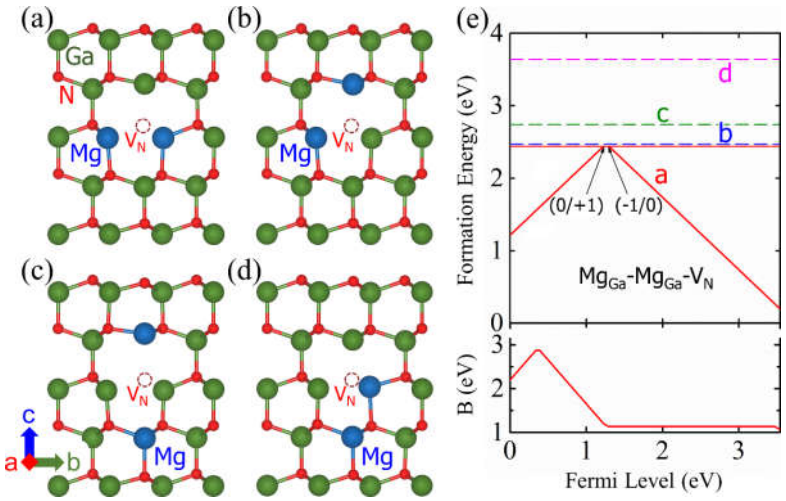

unpublished

Mg_{Ga}-Mg_{Ga}-H_N

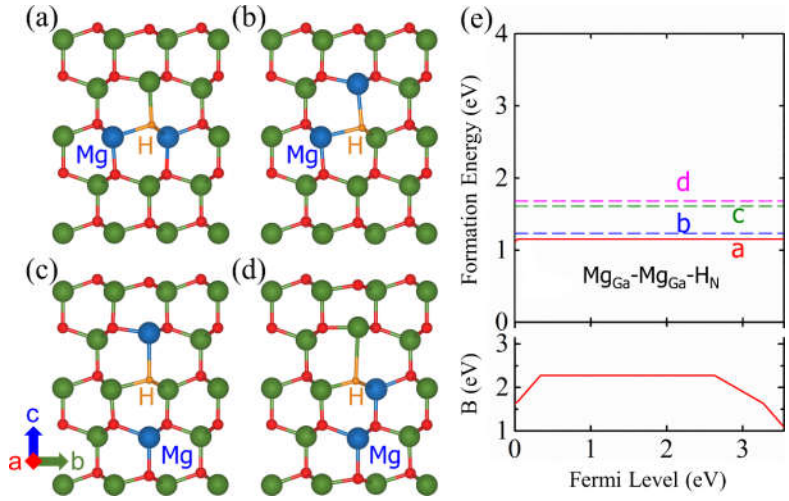

缺陷的光致发光

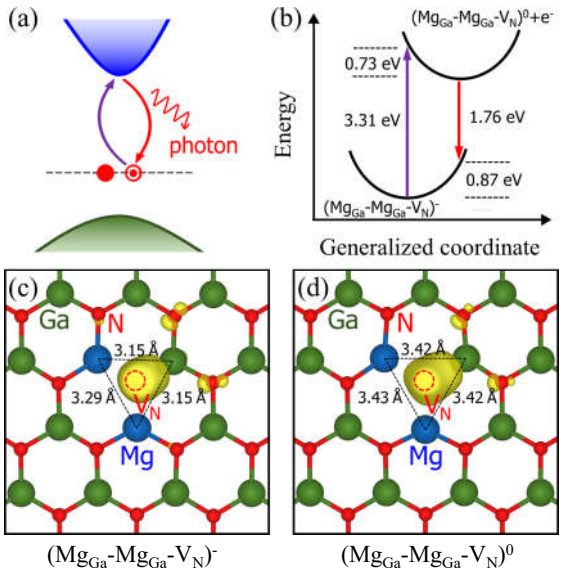

$(Mg_{Ga}\text{-}Mg_{Ga}\text{-}V_N)^-$ $(Mg_{Ga}\text{-}Mg_{Ga}\text{-}V_N)^0$

GaN绿光和红光峰来源缺陷的新解释

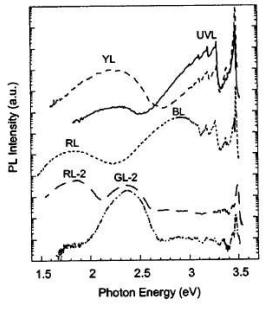

FIG. 13. PL spectra from undoped GaN at 15 K. The spectra are plotted in logarithmic scale and displaced vertically for better viewing.

Yellow luminescence: 2.2 eV

Ultra-violet luminescence: 3.25 eV

Blue luminescence: 2.7-2.9 eV (low temperature)

Red luminescence: 1.8 eV (extremely Ga-rich)

Green luminescence: 2.5 eV (extremely Ga-rich)

M. A. Reshchikov and H. Morkoç, *J. Appl. Phys.* **97**, 061301 (2005)

Blue Luminescence:	Mg_{Ga}	2.7-2.9 eV	C_N: (0/+) C_N+H_i: (0/+)
Ultraviolet Luminescence:	$Mg_{Ga}\text{-}H_i$	3.3 eV	
Green Luminescence:	V_N	2.5 eV	C_NH_N : (+/2+)
Red Luminescence:	$Mg_{Ga}\text{-}V_N$	1.8 eV	C_NV_N: (0/+) $2(Mg_{Ga})+V_N$
Yellow Luminescence:	C_N	2.2-2.3 eV	C_N: (-/0)

程序应用实例2

多元、低对称性半导体光伏材料的点缺陷

光伏半导体的发展趋势

Solar Cell

Device Architecture

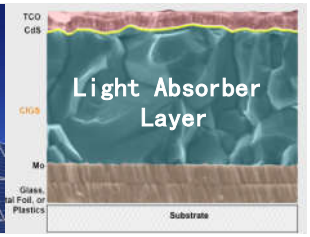

Ideal light absorber

① Band gap: direct, 1.1-1.5 eV
② Suitable band edge
③ High carrier mobility
④ Environment friendly
⑤ Earth abundant, cheap
⑥ …

More and more elements

1950	1960	1970	1980	1990	2000
Si	GaAs	$CuInSe_2$	GaInP/GaAs/Ge	$Cu_2ZnSn(S, Se)_4$	$CH_3NH_3PbI_3$
	CdTe	$CuGaSe_2$			Sb_2Se_3

Crystal Structure Mutation

zincblende-derived **wurtzite-derived**

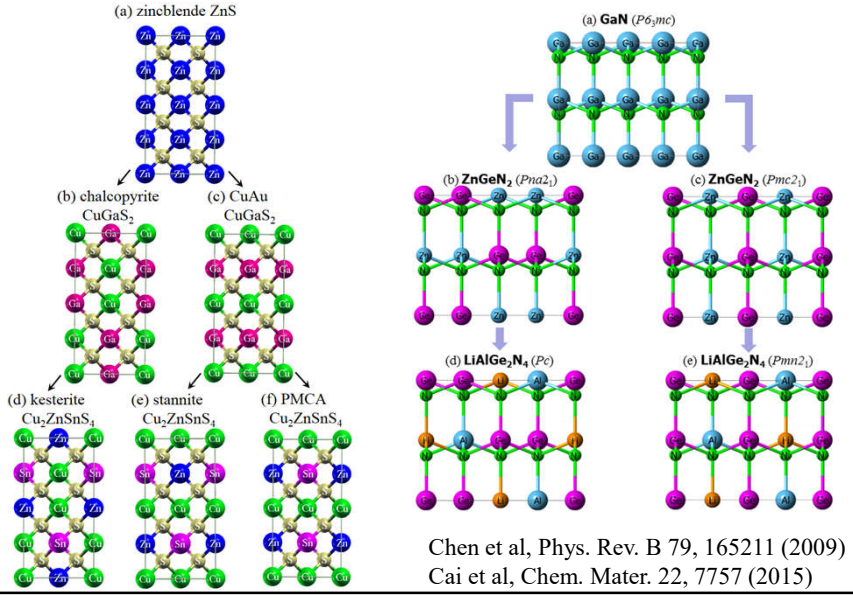

Chen et al, Phys. Rev. B 79, 165211 (2009)
Cai et al, Chem. Mater. 22, 7757 (2015)

Beyond Tetrahedral Coordination

四配位结构
硫族半导体

准一维结构
硫族半导体

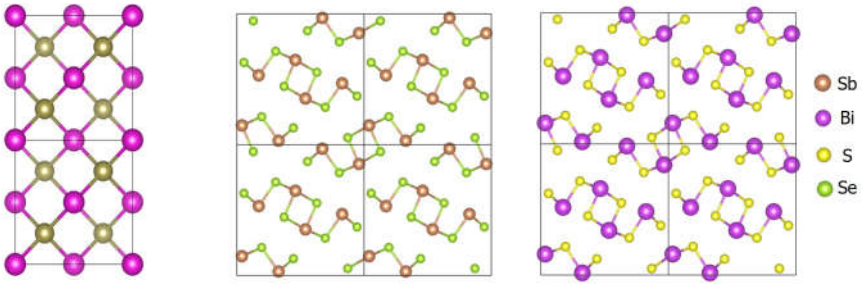

CdTe Sb_2Se_3 Bi_2S_3

高对称性 低对称性

Outline

- $Cu_2ZnSn(S,Se)_4$
- $Cu(In,Ga)Se_2$

多元半导体

- Sb_2Se_3, Sb_2S_3, Bi_2S_3

低对称性半导体
结构多元

Easy formation of Intrinsic Defects

$Cu_2ZnSnSe_4$

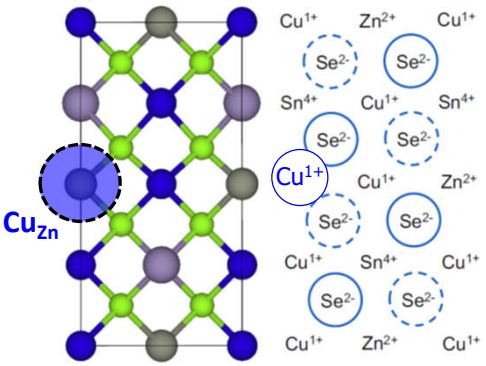

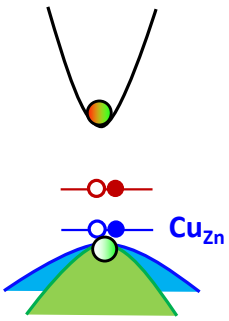

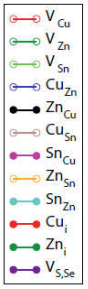

Ionization Levels of Various Defects

Cu_2ZnSnS_4

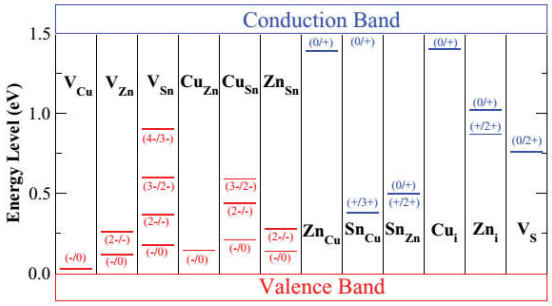

$Cu_2ZnSnSe_4$

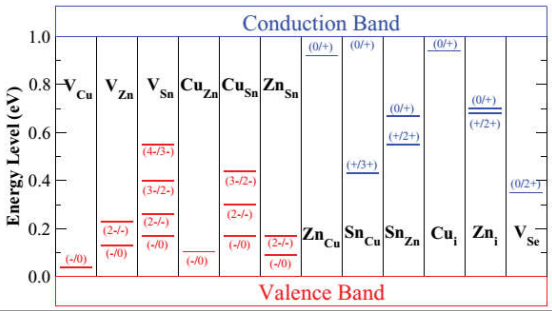

Defect Formation Energies

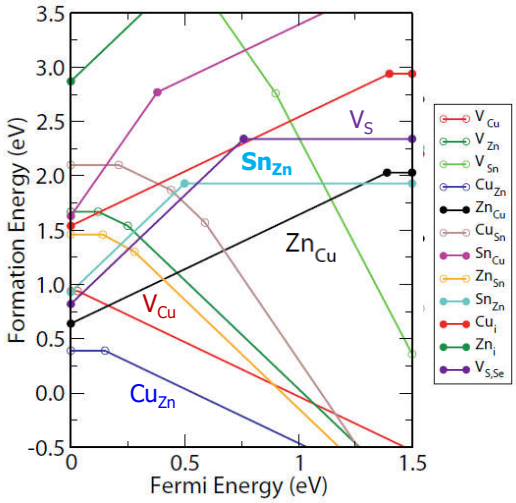

- Accepters have lower energy than donors, explaining the p-type conductivity
- Cu_{Zn} antisite has the lowest formation energy, even lower than V_{Cu}

Chen et al., Adv. Mater. 25, 1522 (2013)
Phys. Rev. B 81, 245204 (2010)
Appl. Phys. Lett. 96, 021902 (2010)

Defect clusters $Cu_{Zn}+Sn_{Zn}$, $2Cu_{Zn}+Sn_{Zn}$

Donor-acceptor passivation

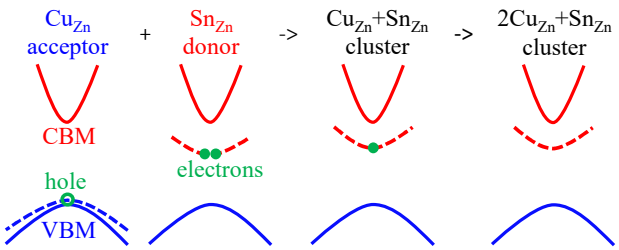

Three factors lower the formation energy:

- donor-acceptor passivation: donor electron goes to acceptor level
- Coulomb attraction between charged donor and acceptor
- strain relief

Chen et al., Appl. Phys. Lett. 101, 223901 (2012)

Band edge shift induced by defect complexes

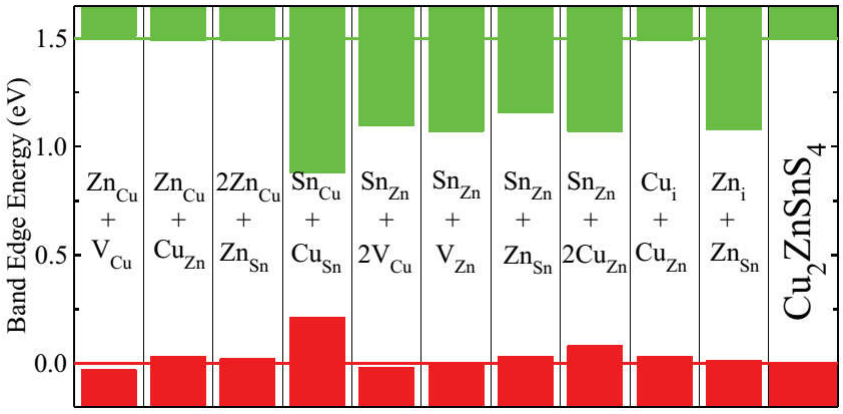

- $V_{Cu}+Zn_{Cu}$, $Zn_{Sn}+2Zn_{Cu}$ do not cause obvious CBM downshift or VBM upshift, and thus do not trap electrons or holes.
- $2Cu_{Zn}+Sn_{Zn}$ causes large CBM downshift, and thus can trap electrons.

Defect and Carrier Concentration

$$\Delta H_\alpha^q(u_{Cu}, u_{Zn}, u_{Sn}, E_F) \rightarrow c_\alpha^q \rightarrow E_F$$

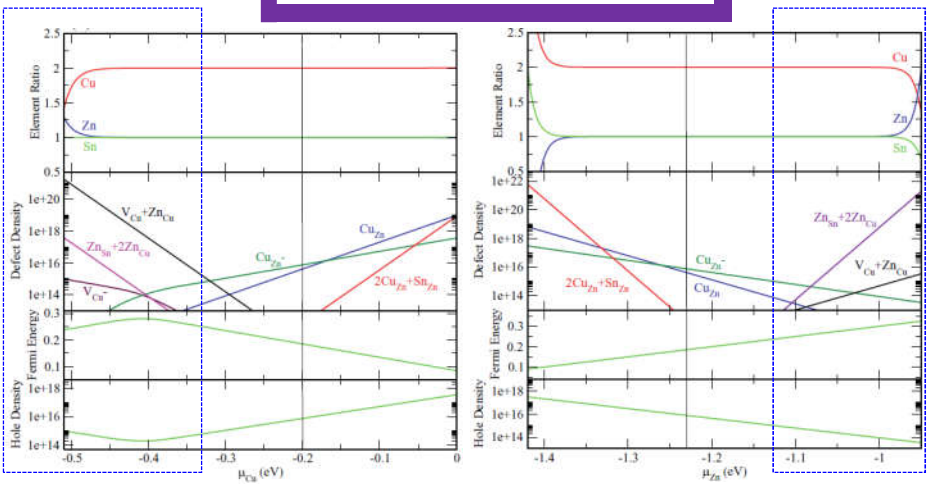

stoichiometric, Cu/(Zn+Sn)=1, Zn/Sn=1: **Cu_{Zn}, $2Cu_{Zn}+Sn_{Zn}$**

Cu poor and Zn rich, Cu/(Zn+Sn)=0.8, Zn/Sn=1.2: **V_{Cu}, $V_{Cu}+Zn_{Cu}$, $Zn_{Sn}+2Zn_{Cu}$**

Non-stoichiometry leads to high efficiency!

Stoichiometric Cu_2ZnSnS_4:
Cu/(Zn+Sn)=1
Zn/Sn=1

High-efficiency solar cells:
Cu/(Zn+Sn)=0.8
Zn/Sn=1.2

Empirical rule:
Cu poor, Zn rich condition is required for high efficiency.

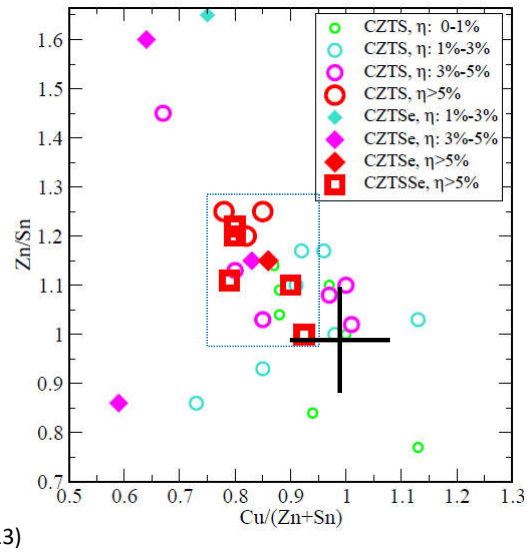

Chen et al., Adv. Mater. 25, 1522 (2013)

Carrier Transition Rate to Defect State

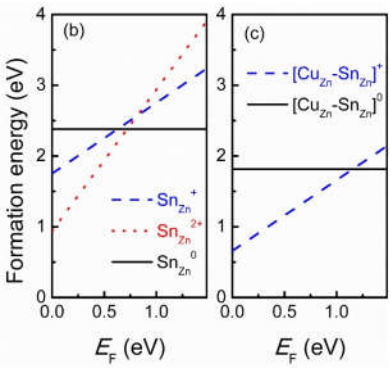

electronic transition rate

$B_e = W_{fi}\, V$

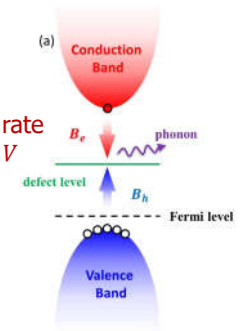

nonradiative decay probability

probability that the system is in the initial phonon state m

electron-phonon coupling matrix elements

$$W_{fi} = \frac{2\pi}{\hbar} \sum_m \sum_n p(i,m) \left| \sum_k \langle \psi_f | \frac{\partial H}{\partial Q_k} | \psi_i \rangle \langle \chi_n | Q_k | \chi_m \rangle \right|^2 \times \delta(\Delta E + E_m - E_n), \quad (1)$$

lattice transition matrix elements between the initial and final phonon states

L. Shi, K. Xu, L.-W. Wang, Phys. Rev. B 91, 205315 (2015)
L. Shi and L.-W. Wang, Phys. Rev. Lett. 109, 245501 (2012)

Calculated Carrier Capture Cross Sections

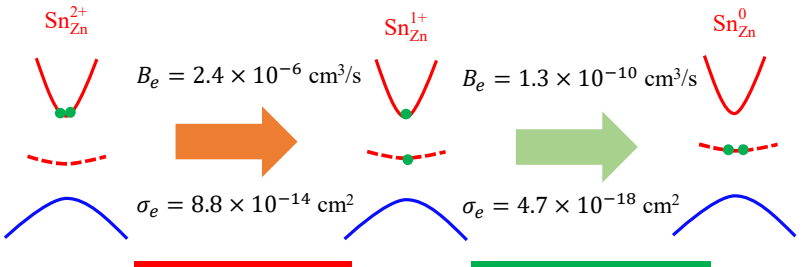

Large Cross Section

Smaller Cross Section

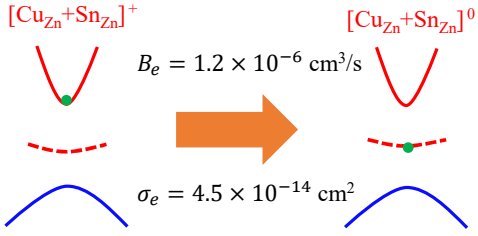

Large Cross Section

- Large cross section when Sn is in +4 charge state,
- Small cross section when Sn is in +3 charge state

Phonons that induce Non-radiate Recombination

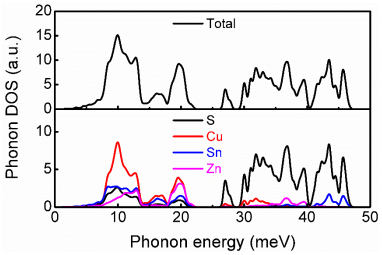

Huang-Rhys factors

electron-phonon coupling matrix elements

transition rates

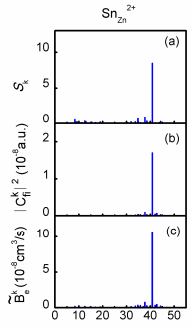

- 41 meV phonon mode is localized around the defect and is the stretching mode of Sn-S bonds
- Overlapping of the defect electronic state and phonon mode, thus strong electron-phonon coupling

$$\left\langle \psi_f \left| \frac{\partial H}{\partial Q_k} \right| \psi_i \right\rangle$$

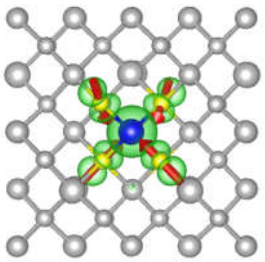

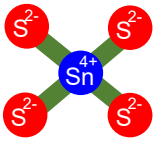

Phonon Mode Softening

Sn_{Zn}^{2+}

$[Cu_{Zn}+Sn_{Zn}]^{+}$

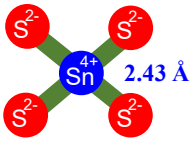

41 meV
phonon mode

Sn 5s state unoccupied

Sn_{Zn}^{1+}

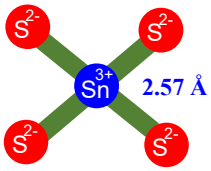

26 meV
phonon mode

Sn 5s state half-occupied

Limit to the Lifetime of Minority Carriers

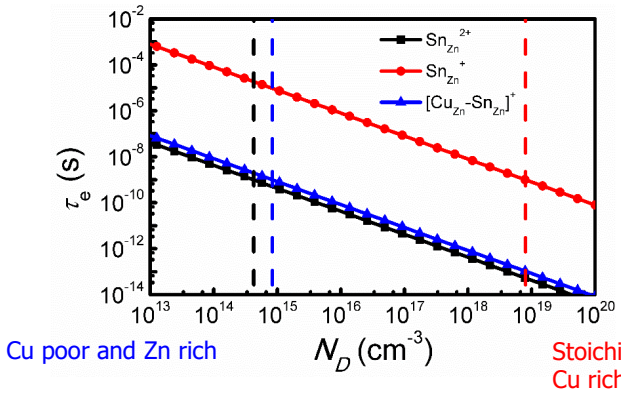

Cu poor and Zn rich

Stoichiometric or Cu rich

◆当这两类复合中心缺陷浓度高于10^{15} cm^{-3}时，少子寿命将短于 1ns

Li, et al. Phys. Rev. B 96, 104103 (2017); Chem. Mater. 31, 826 (2019)

带尾态和深能级复合中心的来源缺陷

J. Phys. Chem. Lett. 2019, 10, 7929−7936

Origin of Band-Tail and Deep-Donor States in Cu_2ZnSnS_4 Solar Cells and Their Suppression through Sn-Poor Composition

Suyu Ma,[†,#] Hongkai Li,[†,#] Jin Hong,[†,#] Han Wang,[†] Xiaoshuang Lu,[†] Ye Chen,[†] Lin Sun,[*,†] Fangyu Yue,[*,†] Jens W. Tomm,[‡] Junhao Chu,[†,§] and Shiyou Chen[*,†]

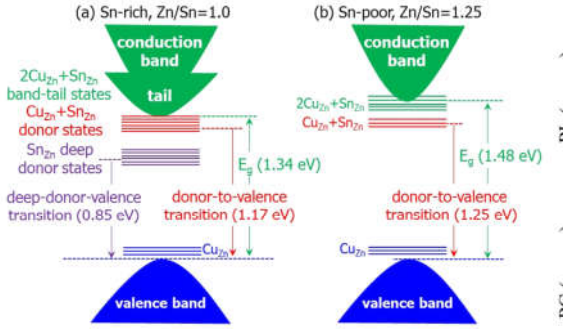

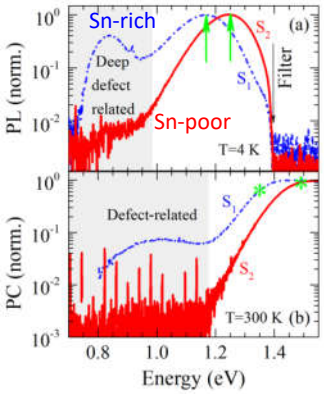

Figure 4. Schematic of the band-tail and donor states induced by Sn_{Zn} and the related defect clusters $2Cu_{Zn} + Sn_{Zn}$ and $Cu_{Zn} + Sn_{Zn}$ in the bandgaps of (a) Sn-rich CZTS with Zn/Sn = 1.0 and (b) Sn-poor CZTS with Zn/Sn = 1.25.

缺陷调控提升太阳能电池效率

Adv. Mater. In press

WILEY-VCH

Defect control for 12.5% efficiency $Cu_2ZnSnSe_4$ kesterite thin-film solar cells by engineering of local chemical environment

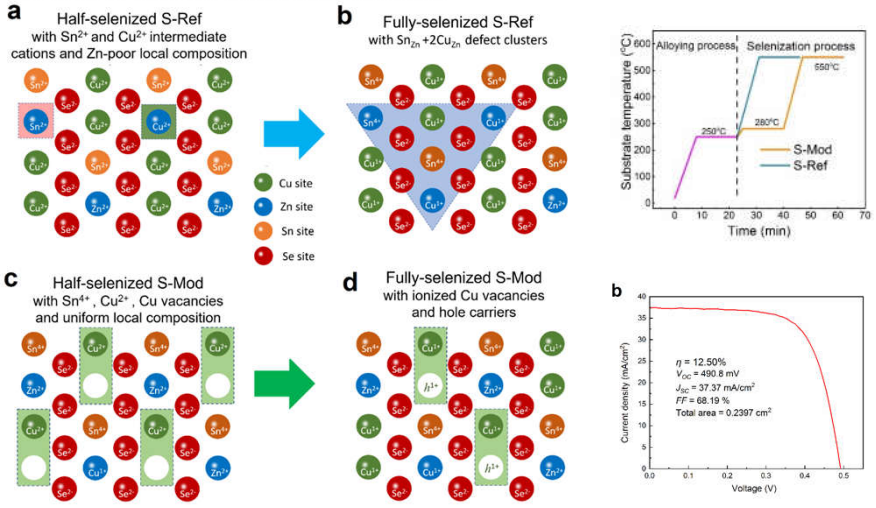

低对称性光伏半导体

$Sb_2(S,Se)_3$ alloys

Sb_2Se_3	1.2 eV
Sb_2S_3	1.6-1.7 eV
Bi_2S_3	1.3-1.45 eV

M. Huang, *et al.* ACS Appl. Mater. Interfaces 11, 15564 (2019)
Z. Cai, *et al.* Solar RRL 4, 1900503 (2020).
D. Han, *et al.* Journal of Materials Chemistry A 5, 6200 (2017)

quasi-1D Semiconductors Sb_2Se_3, Sb_2S_3, Bi_2S_3

Sb_2Se_3, Sb_2S_3, Bi_2S_3

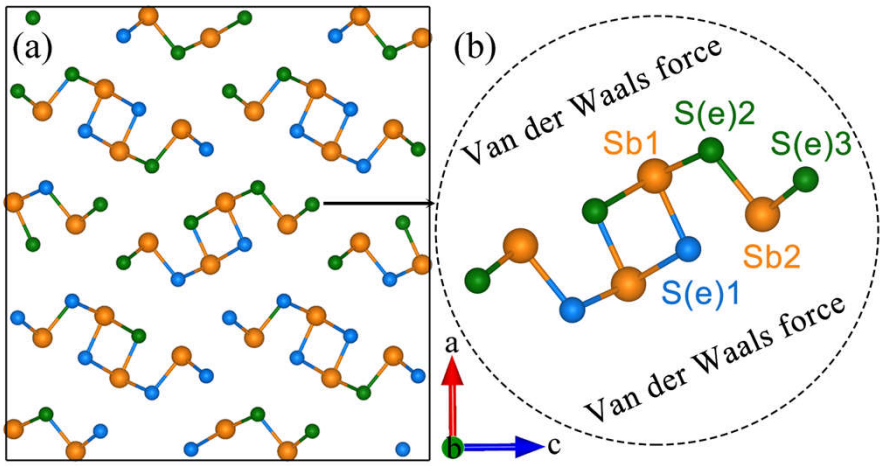

quasi-1D structure

Zhou et al. Nature Photonics 9, 409 (2015)

Highly miscible $Sb_2(S,Se)_3$ alloys

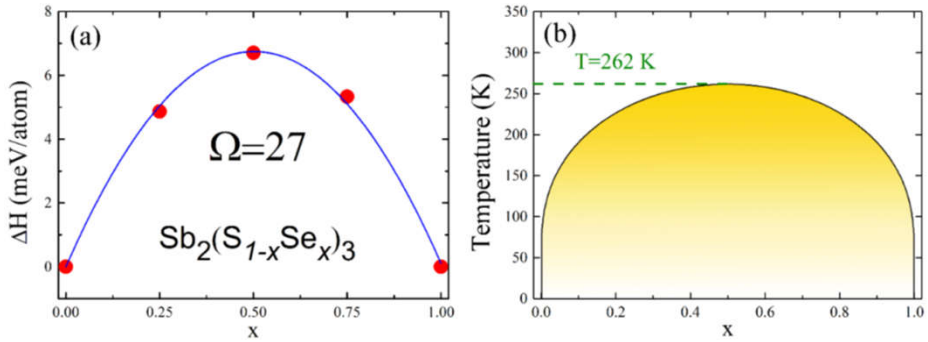

- **The $Sb_2(S,Se)_3$ alloy is highly miscible under room temperature.**
- **The mixing enthalpy is 27 meV/atom (or 45 meV/mixed-atom), lower than that of $Cu_2ZnSn(S,Se)_4$ (52 meV/mixed-atom) and $Cu(In,Ga)Se_2$ (176 meV/mixed-atom).**

M. Huang *et al.*, J. Chem. Phys. 153, 014703 (2020)

Linear dependence of bandgaps on composition

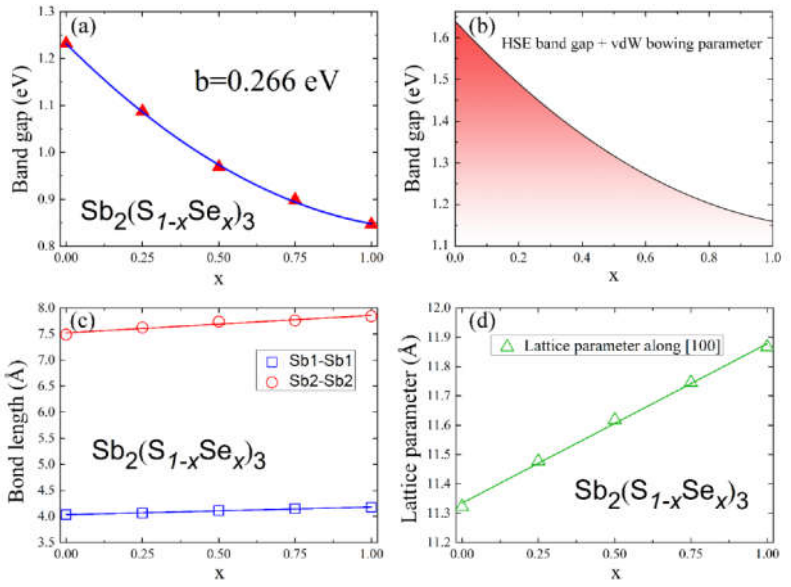

Sb_2Se_3相关无机半导体

$Sb_2(S,Se)_3$ alloys

Sb_2Se_3	1.2 eV
Sb_2S_3	1.6-1.7 eV
Bi_2S_3	1.3-1.45 eV

Very flexible properties,
but many defects!

M. Huang, *et al.* ACS Appl. Mater. Interfaces 11, 15564 (2019)
Z. Cai, *et al.* Solar RRL 4, 1900503 (2020); J. Appl. Phys. 127, 183101 (2020)
D. Han, *et al.* Journal of Materials Chemistry A 5, 6200 (2017)

How many point defects in Sb_2Se_3

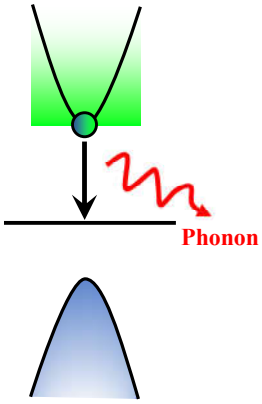

Deep defect levels acting as non-radiative recombination center limit the photovoltaic performance.

Sb_2Se_3

V_{Sb}
V_{Se}
Sb_{Se}
Se_{Sb}
Sb_i
Se_i

Only 6 defects

Cu_2ZnSnS_4

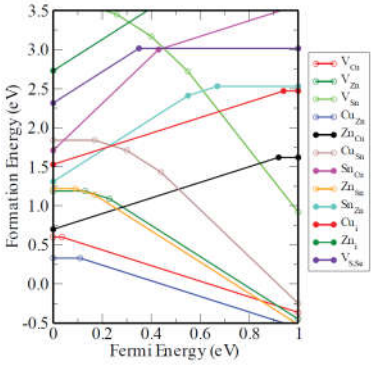

Dozens of defects

X. Liu, et al. Prog. Photovolt. 25, 861 (2017)

Defects at non-equivalent Atomic Sites

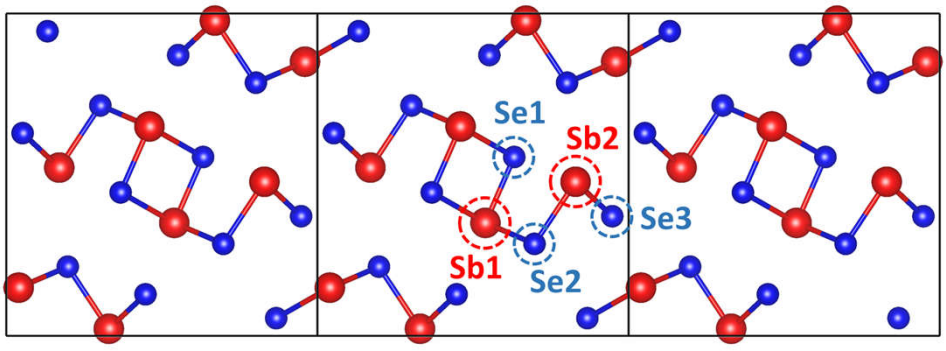

3 Se sites and 2 Sb sites!

Se sites: V_{Se1}, V_{Se2}, V_{Se3}, Sb_{Se1}, Sb_{Se2}, Sb_{Se3}
Sb sites: V_{Sb1}, V_{Sb2}, Se_{Sb1}, Se_{Sb2}

Huang et al. ACS Appl. Mater. Interfaces 11, 15564 (2019)

Three different Se vacancies in Sb_2Se_3

V_{Sb} V_{Se}
Sb_i Se_i
Sb_{Se} Se_{Sb}

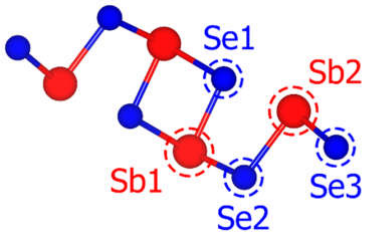

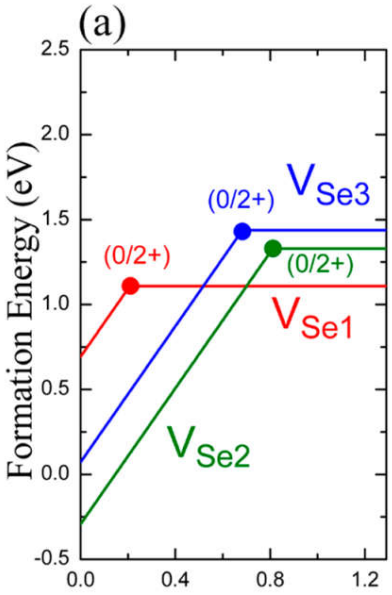

V_{Se} and Sb_{Se}

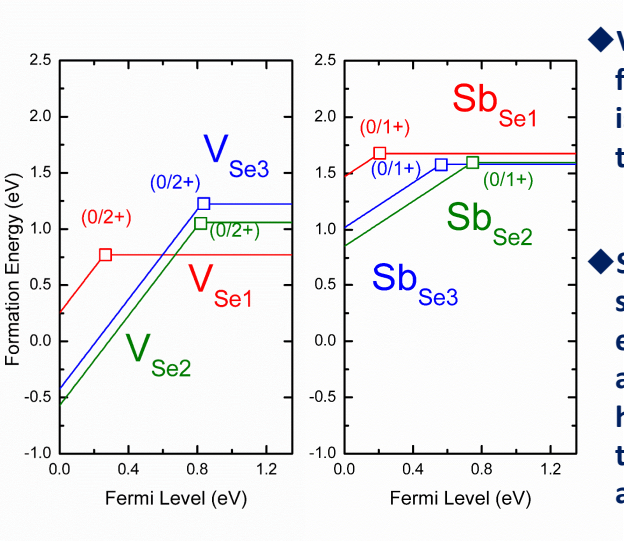

- **V_{Se} is a deep donor for all Se sites: V_{Se1} is much deeper than V_{Se2} and V_{Se3}.**
- **Sb_{Se} has almost the same formation energy for all Se sites at neutral states, however, their transition levels (0/1+) are different.**

Huang et al. ACS Appl. Mater. Interfaces 11, 15564 (2019)

Defects on Different Atomic Sites

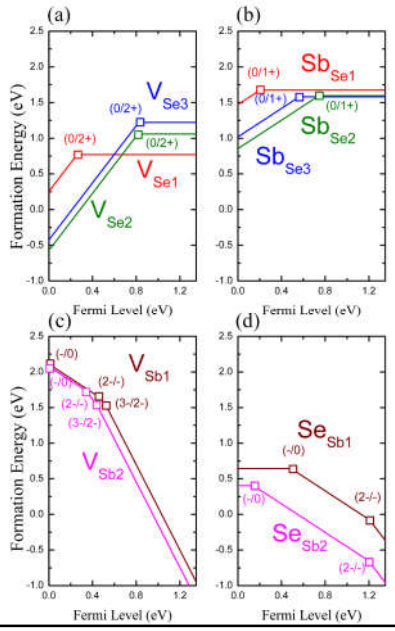

- Defects at non-equivalent sites have quite different properties
- Se_{Sb} and Sb_{Se} antisites can have high concentration
- Se_{Sb} is an acceptor

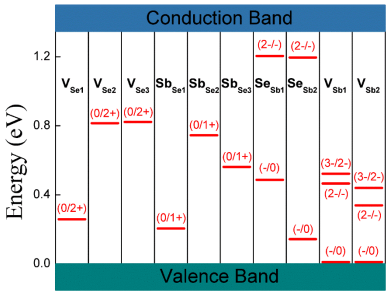

More abnormal defects with high concentration

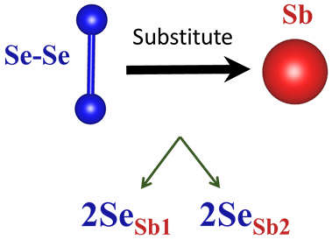

- ***$2Se_{Sb2}$*** *can have high concentration under Se-rich condition.*

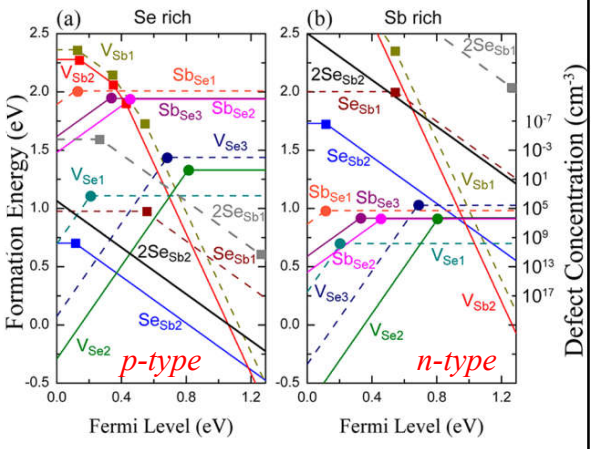

- **There are high concentration of recombination center defects under both the Se-rich and Sb-rich condition, so the passivation of these unavoidable defects may be critical to the further optimization of Sb_2Se_3 solar cells.**
- **Defects are as complicated as those in multinary compounds.**

Non-equivalent defects in Sb_2S_3

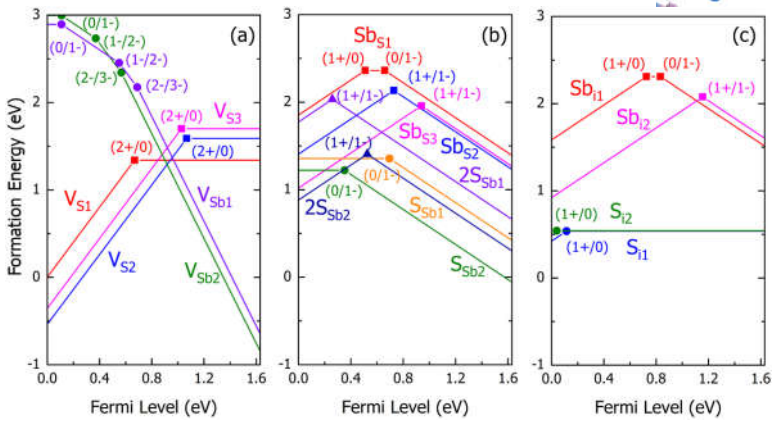

- Cation-replace-anion antisite defects can act as acceptor (Sb_{S1}, Sb_{S2}, and Sb_{S3}).
- Formation energies of antisite defects and S_i can be quite low.
- Defect complexes are easy to form in Sb_2S_3 ($2S_{Sb1}$, $2S_{Sb2}$).

Origins of High Resistivity of Intrinsic Sb_2S_3

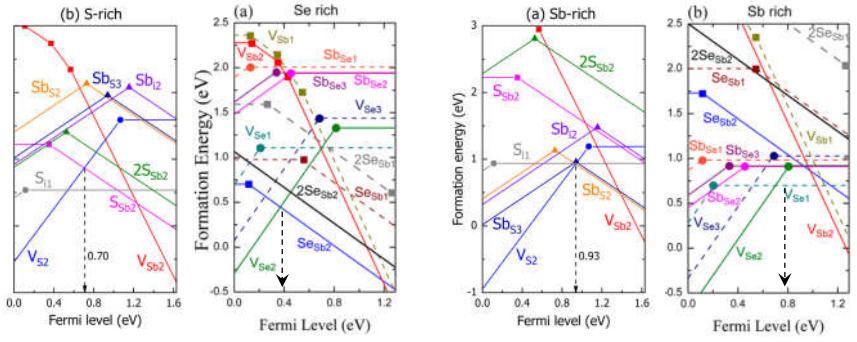

S-rich Sb_2S_3 | Se-rich Sb_2Se_3 | Sb-rich Sb_2S_3 | Sb-rich Sb_2Se_3

poor p-type | *p-type* | *poor n-type* | *n-type*

- High concentration (low formation energy) of deep-level defects.
- The electrical conductivity of Sb_2S_3 is limited by intrinsic point defects.

Z. Cai, *et al.* Solar RRL 4, 1900503 (2020); J. Appl. Phys. 127, 183101 (2020)

Defects in the $Sb_2(S,Se)_3$ alloys

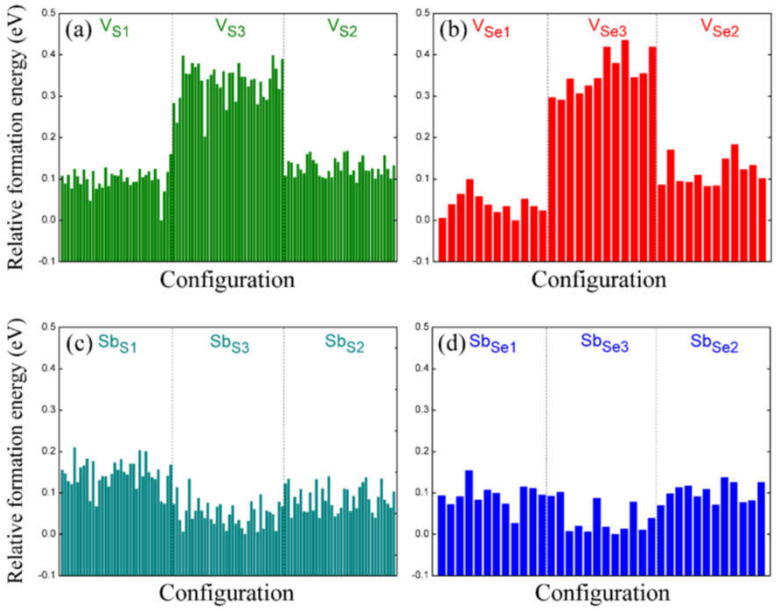

Defect formation energies

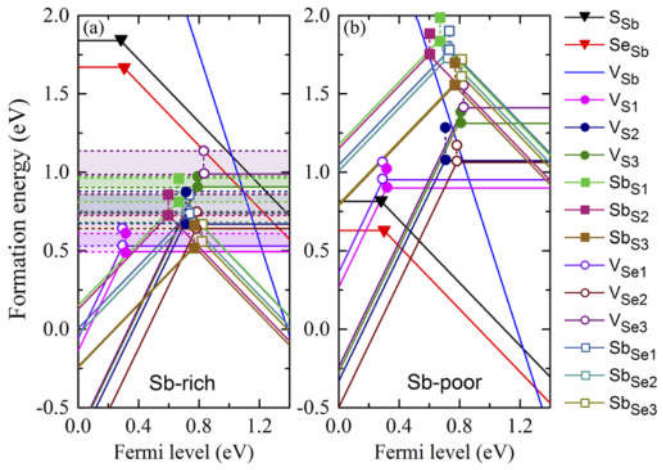

M. Huang *et al.*, J. Chem. Phys. 153, 014703 (2020)
R. Tang *et al.*, Nature Energy 5 (8) , 587-595 (2020)

Strategies for increasing carrier concentration

Unintentional dopants: O impurity

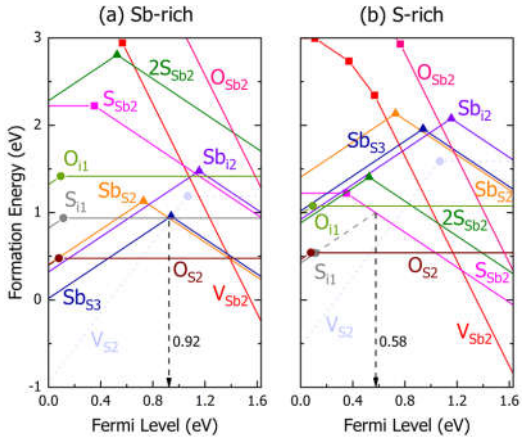

◆ Low formation energy of O_{S2}.

◆ The dominant donor V_{S2} is filled, making the p-type doping easy to be realized.

Strategies for achieving high hole concentration

Method II: Using the unexpected effect of O doping

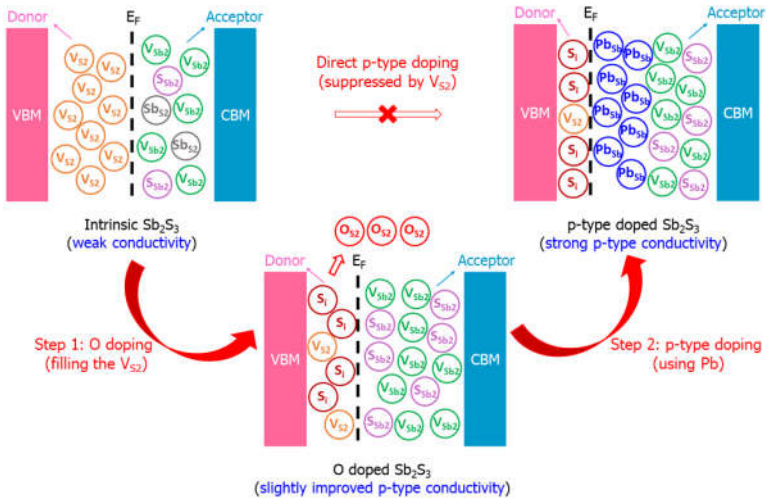

Z. Cai et al., Solar RRL 4, 1900503 (2020).

Intrinsic Defects in Bi_2S_3

Bi-rich **S-rich**

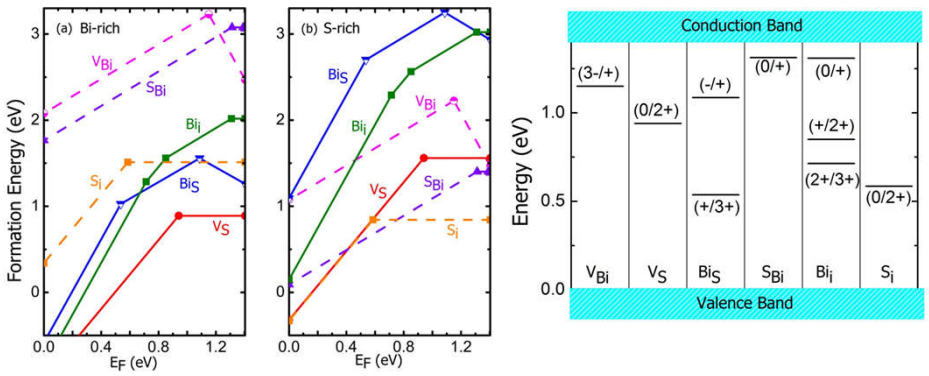

Abnormal characters:

- S_i is a donor, and Sb_S and S_{Sb} have low formation energies, similar to those in Sb_2S_3
- Almost all defects are donors, so Bi_2S_3 is always n-type intrinsically.
- High concentration of deep-level defects, so the minority carrier lifetime is limited and thus Bi_2S_3 is not a good light-absorber semiconductor

Cu, Ag, F, Cl, Br and I doping in Bi_2S_3

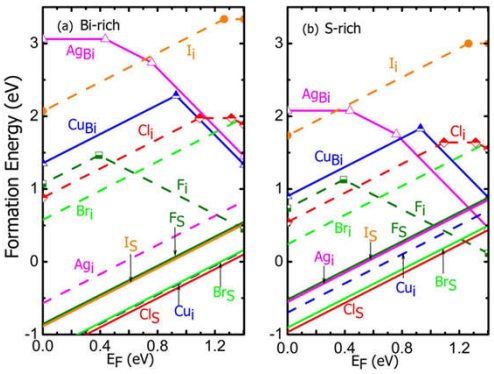

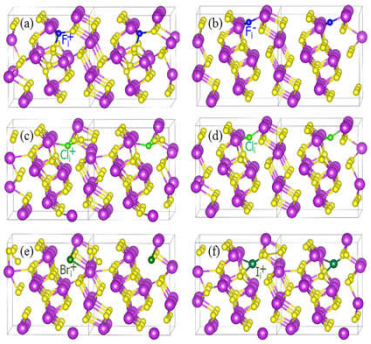

F, Cl, Br and I interstitials between atomic ribbons can also act as donors

- All these dopants prefer acting as donors
  - ① Cu and Ag prefer interstitial sites
  - ② F, Cl, Br and I prefer the anion sites, replacing S
- Very good n-type conductivity can be achieved by doping with Cu, Cl and Br
- Bi_2S_3 may be an ideal n-type electron acceptor or counter electrode material

Band Edge Position and Doping Limit

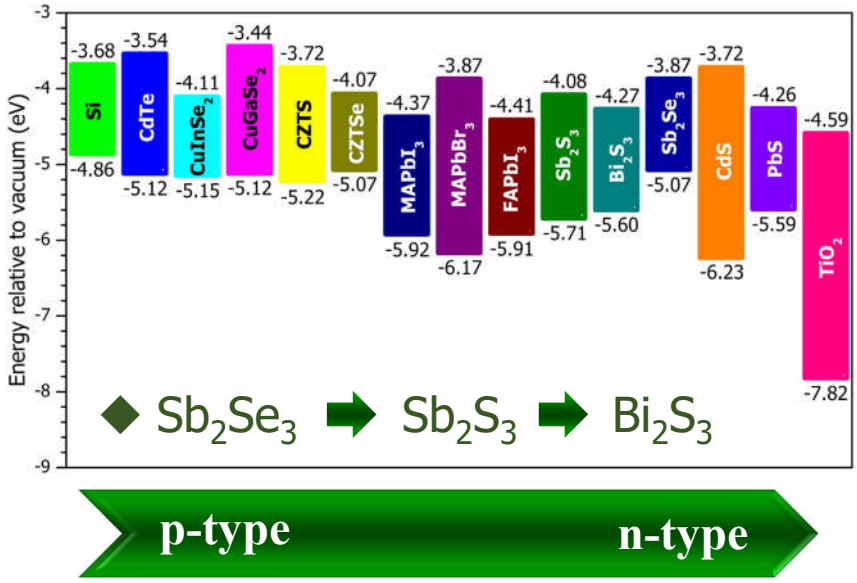

Conclusions

◆ $Cu_2ZnSn(S,Se)_4$ Multinary

Complicated Defects

◆ Sb_2Se_3, Sb_2S_3, Bi_2S_3 Low-Symmetry

Chemically Binary, Structurally Multinary

Complicated Defects

提纲

1. 计算辐照下可能产生的各种缺陷的平衡态性质
   形成能、能级和载流子俘获截面

2. 模拟辐照下化学键的断裂和缺陷形成过程

电子束辐照下半导体缺陷的产生

P-Type Conduction in Mg-Doped GaN Treated with Low-Energy Electron Beam Irradiation (LEEBI)

Hiroshi AMANO, Masahiro KITO, Kazumasa HIRAMATSU and Isamu AKASAKI

Department of Electronics, Nagoya University, Furo-cho, Chikusa-ku, Nagoya 464-01

(Received October 6, 1989; accepted for publication November 8, 1989)

中村修二

JAPANESE JOURNAL OF APPLIED PHYSICS
VOL. 28, NO. 12, DECEMBER, 1989, pp. L 2112–L 2114

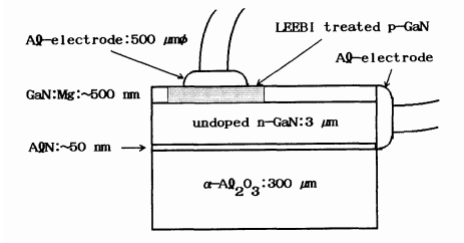

低能电子束辐照导致半导体缺陷的产生和演化，可以提高GaN的p型导电性

The Hall effect measurement of this Mg-doped GaN treated with LEEBI at room temperature showed that the hole concentration is $\sim 2 \cdot 10^{16}$ cm^{-3}, the hole mobility is ~ 8 cm^2/V·s and the resistivity is $\sim 35\ \Omega \cdot$cm. The p-n junction LED using Mg-doped GaN treated with LEEBI as the p-type material showed strong near-band-edge emission due to the hole injection from the p-layer to the n-layer at room temperature.

S. Nakamura, N. Iwasa, M. Senoh, and T. Mukai, Jpn. J. Appl. Phys., Part 1 **31**, 1258 (1992).

电子束辐照对材料的影响

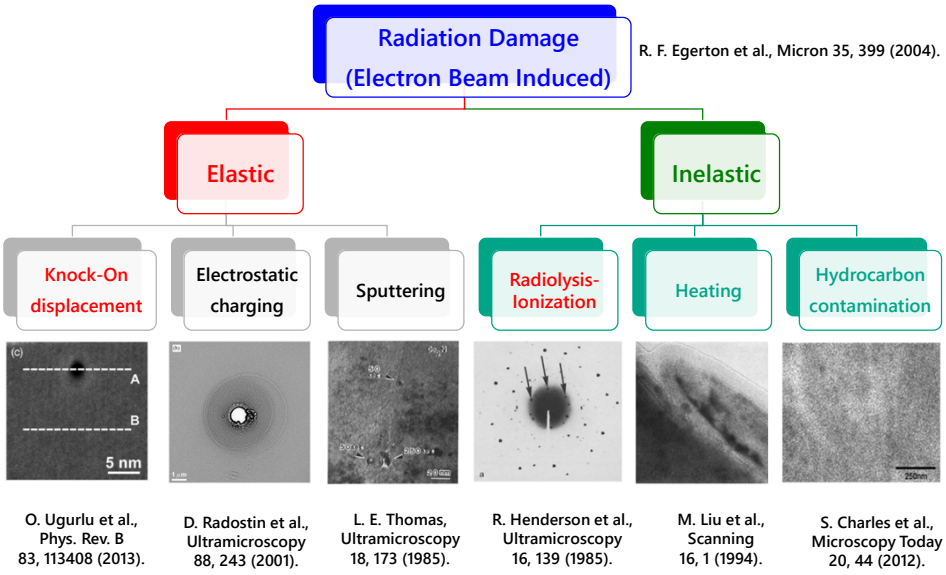

制约TEM技术在有机-无机杂化半导体（$CH_3NH_3PbI_3$）上的应用

电子束辐照引起的两种材料损伤机制

Knock-On Displacement

*Electron-nuclei driven process

*Elastic

→ Inorganic Conducting Materials

Radiolysis-Ionization

*Electron-electron driven process

*Inelastic

→ Inorganic Materials

→ Organic Materials

→ Molecules

R. F. Egerton, Microsc. Res. Tech. 75, 1550 (2012).

电子束辐照引起的两种材料损伤机制

Knock-On Displacement

*Electron-nuclei driven process

*Elastic

Radiolysis-Ionization

*Electron-electron driven process

*Inelastic

Finding the efficient ways to overcome these two main radiation damages is vital to the application of TEM.

Exploring the mechanism behind these two main radiation damages is urgent !!!

R. F. Egerton, Microsc. Res. Tech. 75, 1550 (2012).

Knock-On Displacement

(Molecular Dynamics, MD)

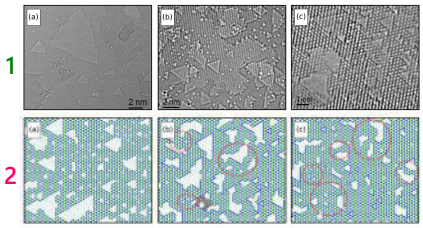

J. Kotakoski et al., Phys. Rev. B 82, 113404 (2010).

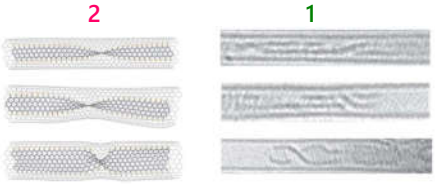

S. T. Skowron et al., Nanoscale 5, 6677 (2013).

TEM Images

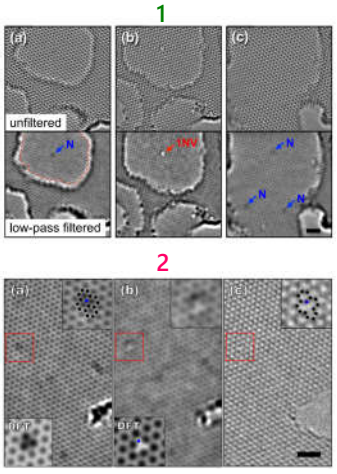

T. Susi et al., ACS Nano 6, 8837 (2012).

MD Simulations

Radiolysis-Ionization Induced Molecule Dissociation

Radiolysis Ionization

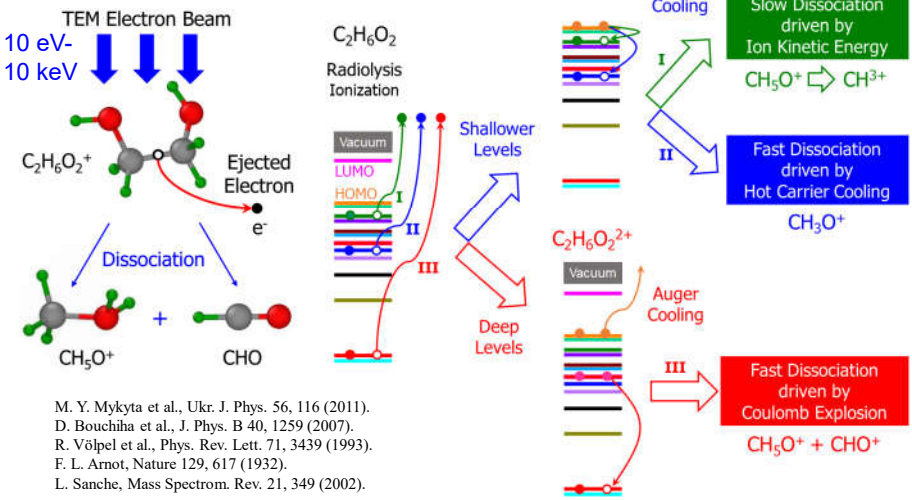

M. Y. Mykyta et al., Ukr. J. Phys. 56, 116 (2011).
D. Bouchiha et al., J. Phys. B 40, 1259 (2007).
R. Völpel et al., Phys. Rev. Lett. 71, 3439 (1993).
F. L. Arnot, Nature 129, 617 (1932).
L. Sanche, Mass Spectrom. Rev. 21, 349 (2002).

Ionization Cross-Section

Binary encounter-dipole (BED) model

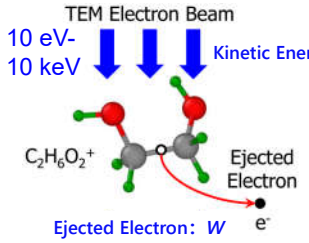

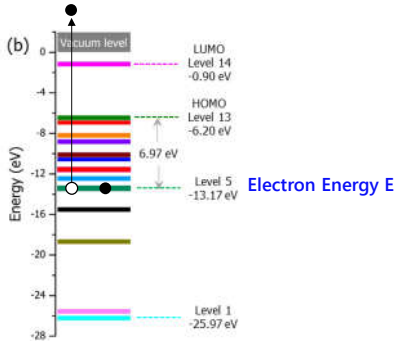

Total Cross Section σ

$$\sigma(t) = \frac{S}{t+u+1}\left[D(t)lnt + (2-\frac{N_i}{N})(\frac{t-1}{t} - \frac{lnt}{t+1})\right]$$

$t = T/E \quad w = W/E \quad u = U/E$

$S = 4\pi a_0^2 N(R/E)^2$

$N_i \equiv \int_0^\infty \frac{df(w)}{dw} dw;$

$$D(t) = N^{-1}\int_0^{(t-1)/2} \frac{1}{w+1}\frac{df(w)}{dw}dw$$

$$\frac{df(w)}{dw} = N/(w+1)^2$$

$$\frac{df(w)}{dw} = (E(w+1)/R)\,(qa_0)^{-2}\textstyle\sum_\Omega |\epsilon(q)|^2$$

$$\epsilon(q) = <\phi 1|\textstyle\sum_{j=1}^{z} \exp(i\vec{q}\cdot\vec{r_j})\,|\phi 0>$$

Y.-K. Kim et al,. Phys. Rev. A 50, 3954 (1994).
M. Inokuti, Rev. Mod. Phys. 43, 297 (1971).

Calculated Ionization Cross-Section

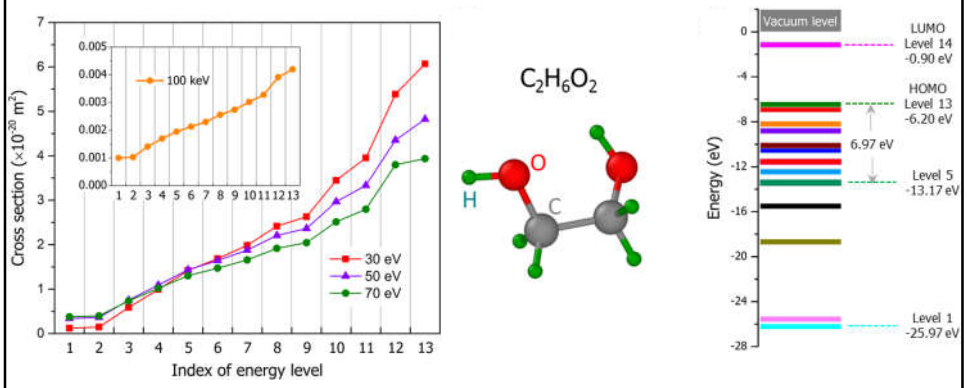

- ❖ Decreasing monotonously from Level 13 to Level 1.
- ❖ Decreasing as the energy of the incident electron beam increases, except for the very deep levels (Level 1-4).
- ❖ Quite small for the high energy electron beam due to the short passing time.

Simulating Radiolysis-Ionization Induced Molecule Dissociation

Radiolysis Ionization

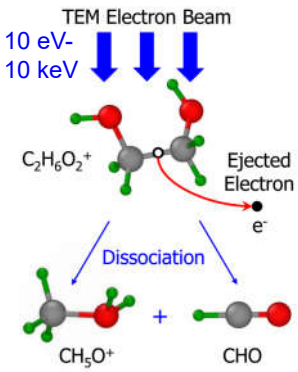

Hot carrier cooling

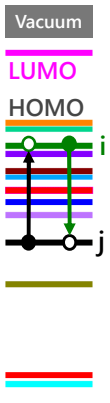

PWMAT

rt-TDDFT

(Ehrenfest Dynamics)

Detailed Balance Restored

Decoherence Restored

J. Kang et al., Phys. Rev. B 99, 224303 (2019).

Hot hole Cooling

Ehrenfest Dynamics Simulation

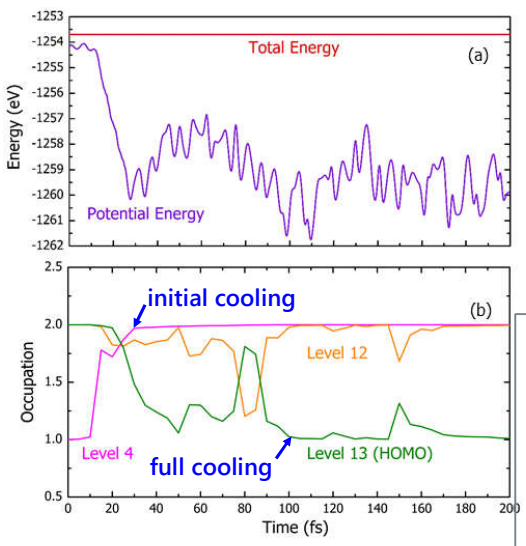

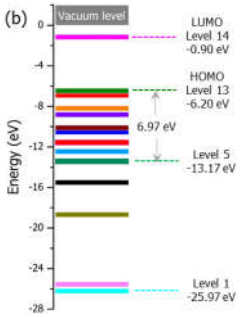

- The released energy is converted to the nuclear kinetic energy.
- The occupation for Level 4 gets back to 2 very quickly (35 fs, initial cooling time).
- The occupation of Level 13 (HOMO) decreases to 1 (100 fs, full cooling time).

Cooling and Dissociation Time

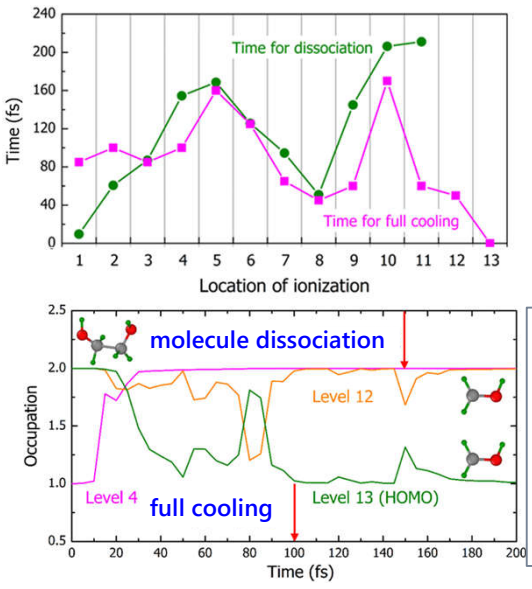

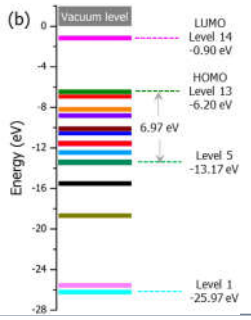

- The dissociation time and cooling time are close to each other.
- The large kinetic energy increase (contributed by the hot hole cooling) plays a significant role.
- No dissociation for Level 12 and 13 ionization

Dissociation Fragments

Ionization Level	Dissociation to different fragments
1	$C_2H_6O_2^+ \rightarrow C_2H_5O^+ (CH_3CHOH^+) + OH$
2	$C_2H_6O_2^+ \rightarrow C_2H_5O^+ (CH_2CH_2OH^+) + OH$
3-11	$C_2H_6O_2^+ \rightarrow CH_3O^+ + CH_3O$
12-13	No dissociation observed

- Highest peak of CH_3O^+: explained
- $C_2H_5O^+$: strange, less at high energy beam energy.

Mass Spectra

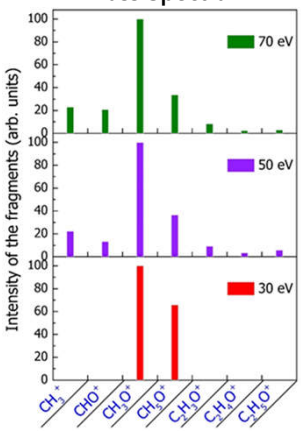

M. Y. Mykyta et al., Ukr. J. Phys. 56, 116 (2011).

Auger Decay

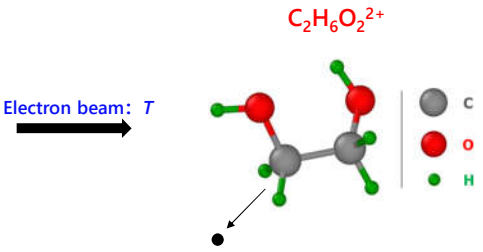

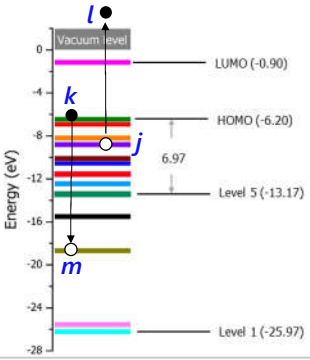

Auger Decay Rate

$$\tau^{-1} = \frac{\Gamma}{\hbar}\sum_{l}\frac{|J(j,k,l,m)|^2}{(\Delta E)^2+(\Gamma/2)^2}$$

L.-W. Wang et al., Phys. Rev. Lett. 91, 056404 (2003).

$$J(j,k,l,m) = \iint \phi_j^*(r,\beta)\phi_k^*(r',\alpha)\frac{e^2}{|r-r'|}\phi_l(r,\beta)\phi_m(r',\alpha)d^3r d^3r'$$

$$\Delta E = E(k) - E(m) + E(j) - E(l)$$

phonon broadening factor $\Gamma = 30$ meV

Time for Auger Decay

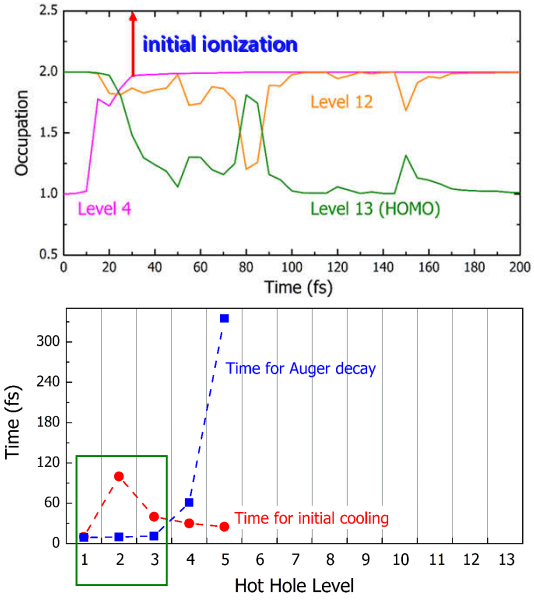

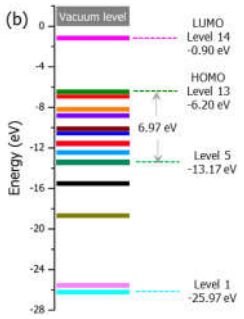

Auger decay can happen at Level 1, 2, 3

Coulomb Explosion

Auger Induced Dissociation

$C_2H_6O_2^{2+} \Rightarrow CH_5O^+ + CHO^+$ $C_2H_6O_2^{2+} \Rightarrow CH_3O^+ + CH_3O^+$

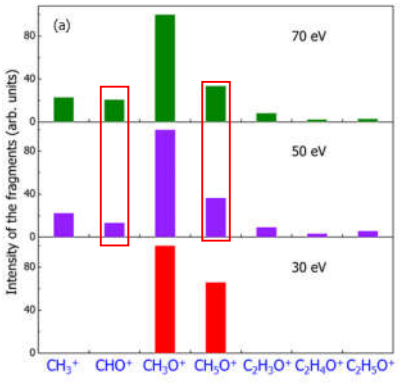

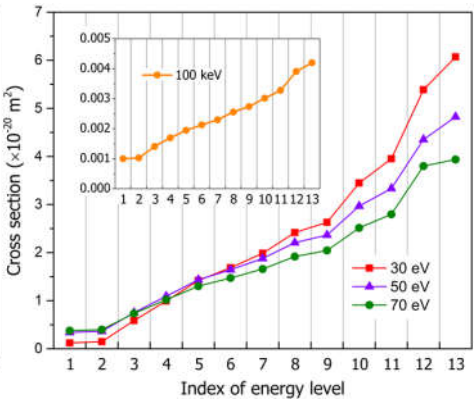

$C_2H_6O_2^+ \rightarrow C_2H_5O^+ + OH$ ✖

$C_2H_5O^+$ is not produced due to the Auger decay

Slow Thermodynamic Dissociation

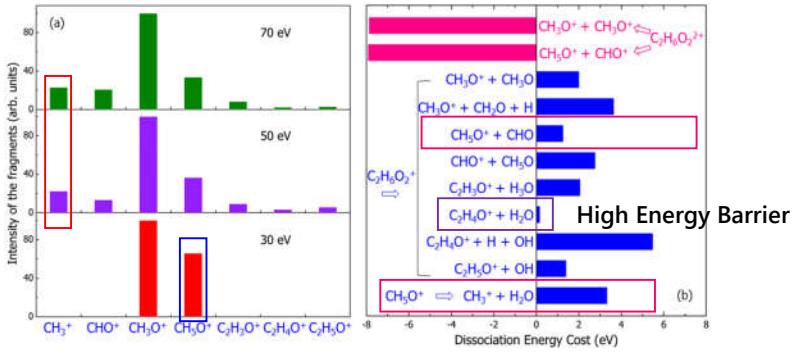

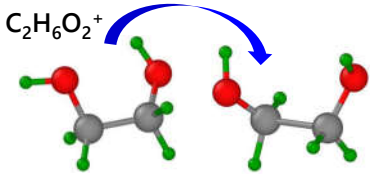

- **Structure reorganization energy**
- **Kinetic energy from hot carrier cooling**

Mass Spectra of Dissociation Fragments

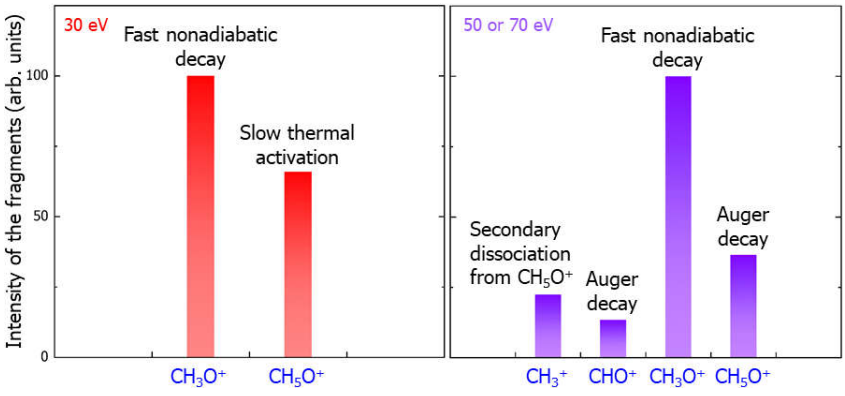

The underlying mechanisms of the main peaks to different dissociation channels under the illumination of electron beams with different incident energies is assigned.

Cai *et al.* Chem. Sci. (2019) DOI: 10.1039/C9SC04100A

TEM中离化分子的多种分裂机制相互竞争

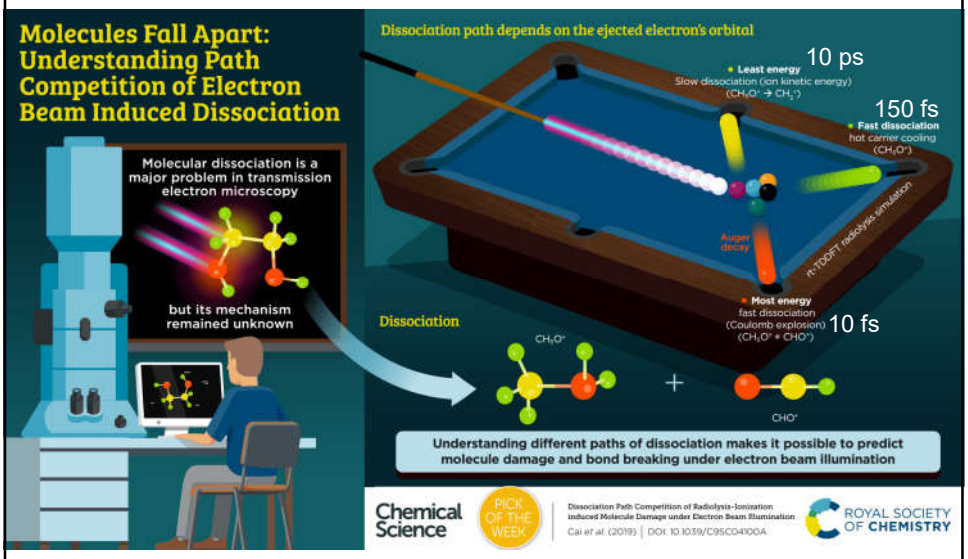

Chemical Science编辑图解

Method Framework for Simulating Radiolysis-Ionization

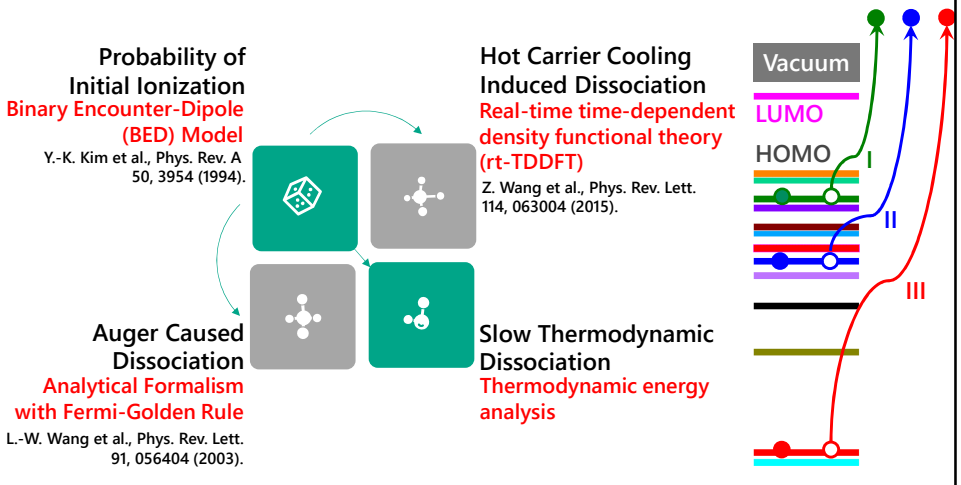

Cai *et al.* Chem. Sci. (2019) DOI: 10.1039/C9SC04100A

提纲

1. 计算辐照下可能产生的各种缺陷的平衡态性质
   形成能、能级和载流子俘获截面

2. 模拟辐照下化学键的断裂和缺陷形成过程

Acknowledgement

Thank you!

国家自然科学基金委员会 National Natural Science Foundation of China

工信部重点研发计划